DEVELOPMENT OF ANTAGONISTICALLY ACTUATED ACTIVE JOINTS WITH SHAPE MEMORY ALLOYS

A Thesis

by

Ali Vahidyeganeh

Submitted to the
Graduate School of Sciences and Engineering
in Partial Fulfillment of the Requirements for
the Degree of

Master of Science

in the
Department of Mechanical Engineering

Özyeğin University
January 2017

DEVELOPMENT OF ANTAGONISTICALLY ACTUATED

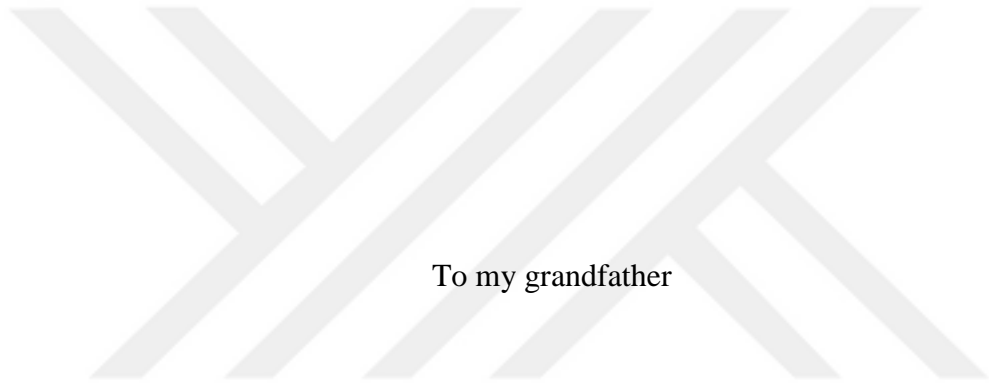# ACTIVE JOINTS WITH SHAPE MEMORY ALLOYS

Approved by:

_____

Associate Professor Güney Güven Yapıcı,
Advisor
Department of Mechanical Engineering
Özyeğin University

_____

Assistant Professor Özkan Bebek,
Department of Mechanical Engineering
Özyeğin University

_____

Assistant Professor Mehmet İpekoğlu,
Department of Mechatronics Systems
Turkish German University

Date Approved: 27 December 2016

To my grandfather

ABSTRACT

The focus of this research work is the development of an active joint antagonistically actuated by shape memory alloys (SMA). Due to their high force to mass ratio these identified as excellent actuator candidates for biomedical, robotic, aerospace and automotive applications. Specifically, NiTi alloys attract attention because of their unique features such as relatively high transformation temperature and recoverability of strain values up to 8%. This study is intended to exhibit the development of antagonistically actuated active joints supported by a thorough understanding of their behavior. Cyclic tests of the active joint have been conducted at various angle amplitudes. The results showed that number of cycles to failure considerably reduced by an increase in the target angle amplitude such that actuation ceases over 100°. It was found that higher peak temperatures of the actuator elements were needed to reach the same bending angle within the subsequent cycles. This observation was attributed to possible increased localized deformation around the martensite plates resisting phase transformation. It was also seen that in resting stages between the actuation durations of opposing elements, a reverse deformation takes place, which remarkably rose with the increase in cycle numbers. This observation was linked with elevated stress levels and the increased resistance by the antagonist actuator, resulting in the greater peak temperature in consecutive cycles. Further investigations also provide a gradually ascending trend of transformation temperatures and stress hysteresis as implication of the cyclic response.

ÖZETÇE

Bu çalışmada tersinir etkili şekil hafızalı alaşımların aktüatör olarak kullanıldığı bir eklem geliştirilmiştir. Şekil hafızalı alaşımlar, kütlesine oranla çok yüksek kuvvetler üretebildiğinden biyomedikal, robotik, uzay ve otomotiv sektörlerinde tercih edilen aktüatör elemanlarındandır. Özellikle NiTi alaşımları yüksek faz dönüşüm sıcaklıkları ve %8'e varan gerinme toparlanması gibi eşsiz özellikleri ile dikkat çekmektedir. Bu çalışmada NiTi alaşımlarının davranışlarının kapsamlı anlaşılması ile desteklenen ve tersinir etkili aktüatörlerle oluşturulan bir eklem tasarımı gösterilmektedir. Aktif eklemin çevrim testleri farklı açılar temel alınarak gerçekleştirilmiştir. Elde edilen sonuçlar, 100º ve üzeri gibi büyük açılar hedeflendiğinde, çevrim sayılarının azaldığını göstermektedir. Öte yandan aktüatör elemanlarının devam eden döngülerde aynı eğme açısına ulaşılabilmesi için yüksek sıcaklık değerlerine erişimin gerektiği gözlemlenmiştir. Bu gözlemler, faz dönüşümünü engelleyici nitelikte ortaya çıkan martensit plakaları çevresindeki olası bölgesel deformasyonlardaki artışla açıklanabilir. Ayrıca eklemde karşıt çalışan elemanların aktüasyon süreleri arasındaki bekleme evrelerinde, döngü sayısı ile birlikte önemli ölçüde artan tersine şekil değişimi görülmüştür. Bu gözlem, ileri döngülerdeki yüksek gerilme seviyeleri ve tersinir aktüatörün artan direnci sebebiyle ortaya çıkan yüksek tepe sıcaklık değerleri ile ilişkilendirilmiştir. Yapılan çalışmalar, faz dönüşüm sıcaklıkları ve gerilme histerezis değerlerindeki artışın çevrimsel yük altında tepkinin göstergesi olduğunu belirtmiştir.

ACKNOWLEDGEMENTS

TABLE OF CONTENTS

LIST OF TABLES

LIST OF FIGURES

CHAPTER I

1. INTRODUCTION

1.1.   Background of the work

First step for discovery of shape memory alloys (SMA) was taken by Adolf Martens in 1890s, when he discovered martensite phase in steel, which led to intensive investigation of martensite transformation in the early 20th century [1]. Chang and Read recorded a case of shape memory transformation in 1932 in metallography of AuCd. By 1951 macroscopic shape memory behavior was presented in a bent bar of AuCd [2]. In these cases of steel, the occurring martensitic transformation were known to be irreversible. It was Kurdjumov and Khandros to observe reversible martensitic transformation in CuZn and CuAl alloys in 1949 for the first time and present the thermoelastic martensitic transformation in order to explain this phenomenon. In the following years researchers observed thermoelastic martensitic transformation in InTl and CuZn alloys as well [1].

In 1963, W. J. Buehler and his coworkers, successfully developed a NiTi alloy for heat shielding in the space program at the Naval Ordnance Laboratory in Silver Springs of Maryland. This discovery was a turning point, which paved the way for first utilizations of shape memory alloys in industries. This innovative NiTi alloy, in addition to comparable mechanical properties to other engineering metals, is capable of recovering its shape when undergone specific heat treatment and annealing procedure. This shape recovery was then referred to by the term Shape Memory Effect (SME) and this group of alloys which demonstrate super-elastic or shape recovery behavior were named Nitinol which serves as an acronym for the component metals, Nickel and Titanium and Naval Ordnance Laboratory. Discovery of Nitinol resulted in spike of research interest in SMAs. In the

coming years after 1963, effects of heat treatment and microstructure were investigated [1,3].

Shortly after the introduction of Nitinol it was discovered that addition of a third element to the alloy results in considerable decrease of transformation temperatures. Cryofit which was the first commercial application of SMAs in Bobcat fighters, was inspired by these new alloys, consisting a third element [4]. Due to low transformation temperature of Cryofit, it was transported in liquid nitrogen before assembly. By 1970, alloys with transformation temperatures higher than boiling point of water (TiPd, TiPt, TiAu) were generated and called high temperature SMAs. Years after, in 1989, NiTiNb alloys were developed to provide higher temperature hysteresis and be easier to handle. These new alloys gained popularity in damage repair systems such as in nuclear reactors. Further fatigue investigation by Melton and Mercier (1978), disclosed that adding copper as the third element does not change transformation temperatures but result in smaller hysteresis of stress; and Miyazaki presented new results in 1999, confirming better fatigue behavior for NiTiCu. This scientific finding then increased demand for these alloys in more industrial and commercial products [1].

Industrial presence of NiTi began with its use in biomedical instruments in the 1970s, and by the 1990s these alloys made their way to the marketed innovative products. By 1990s NiTi alloys had begun to appear in air conditioning and electrical connection industries as well as valve manufacturing. Boeing financed researchers working on SMAs, such as Variable Geometry Chevron, in which SMA is used to deform the chevron in the fan structure of the Boeing 777 engine. This has resulted in decreased noise and vibration [5]. By the beginning of the new millennium, high demand in actuation at higher temperatures, brought about a new wave of interest in high temperature SMAs from the petroleum and aerospace sector [1].

2

In the past decades, more researchers spent time on developing reliable constitutive models for the behavior of these alloys, since over the initial 40 years of their existence in research topics there has not been enough progress in this aspect. During the early decades of research on NiTi alloys a good understanding of their micromechanics has been accumulated [6]. The complexity of the relations between microscopic and macroscopic properties of these alloys has been driving the researchers in the past two decades. This complexity is a result of the different behavior of these alloys according to external triggers such as temperature change or loading [6].

1.2. *Definition of shape memory alloys*

A shape memory alloy such as Nitinol has the distinct characteristic of being available in two temperature-dependent phases. In lower temperatures the crystal structure is referred to as martensite and in high temperatures it is known as austenite which is the parent phase [7]. This parent phase has a stable crystalline of body-centered cubic lattice (Figure 1). Cooling the alloy passing a gateway temperature range will induce a change of crystal structure of the alloy which is coined as martensitic transformation. Resulted phase is also often called the daughter (martensite) and is the consequence of a shear process [3]. Martensite in turn is comprised of a monoclinic B19' lattice [8] (Figure 2). While, the macroscopic shape of the alloy is reserved the martensite phase is called twinned martensite phase (Figure 1).

Properties of Nitinol such as stiffness, resistivity and yield strength are prone to surmountable changes in value, when temperature changes through the transformation temperature values. When cooling, these values make up a range from the martensite start to finish temperatures. Consequently, the opposite occurs while heating up through the austenite start and finish temperatures.
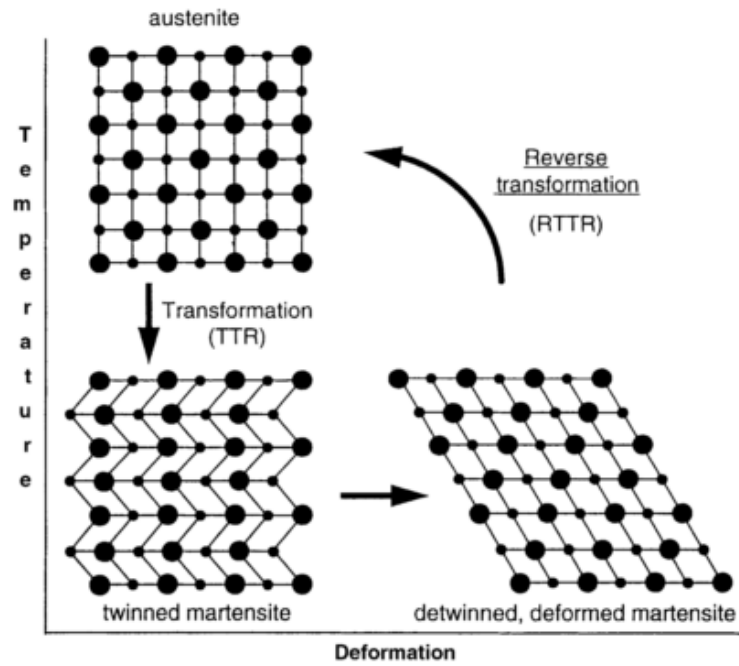
Figure 1. Representation of martensitic transformation and shape memory effect [3]
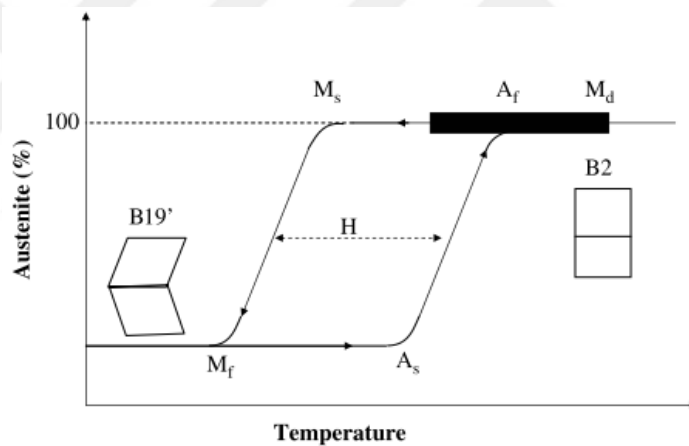
Figure 2. Phase transformation in NiTi [8]. The heavy block shows the temperatures in which superelasticity is observed.

Differential scanning calorimetry (DSC) facilitates monitoring transformation of an alloy through different phases. Simultaneously, physical and mechanical behavior of the alloy can be studied for observing transformation process as well. Figure 3, demonstrates an example DSC result graph in which Nearly equiatomic is heated up to 100°C and cooled down back to -70°C. Endothermic transition of martensite to B2 lattice of austenite is depicted as the peak between austenite start (A_s) and austenite finish (A_f) temperatures [7].

4

The enveloped area under this peak also equals the latent transformation heat. In some cases, an intermediate phase which is referred to as R (rhombohedral lattice) occurs before full transition of crystal from austenite to martensite which is shown as the first exothermic valley in the cooling graph [6].
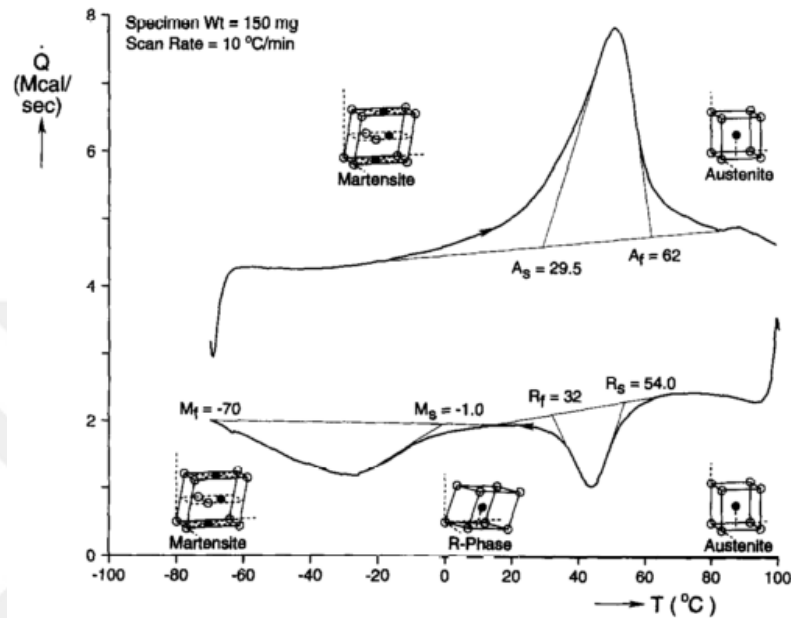
Figure 3. Differential scanning calorimetry thermogram for NiTi [6]

The above-mentioned transformation temperatures are to be manipulated with changing the composition of the alloy. Adding other elements to the mixture can result in higher or lower critical temperatures. As CuAlNi alloys exhibit austenite finish at temperatures up to 200°C [9].

One of the characteristics of the martensite phase is it being more ductile than austenite, hence exerting a shear stress will deform the alloy. This process is then called de-twinning of the alloy. This deformation is recovered when the alloy is heated. Increase in temperature will trigger the transformation of crystal structure back to austenite body centered cubic lattice which as mentioned before possesses stable energy (Figure4). This repossession of original parent shape is then called shape memory effect (SME). It is important to have in mind that total atomic movement between neighboring atom planes is less than an

5

interatomic distance in the normal lattice structure. SME is a result of directional electron bonds which drive the atoms back to their original places when thermally triggered [3]
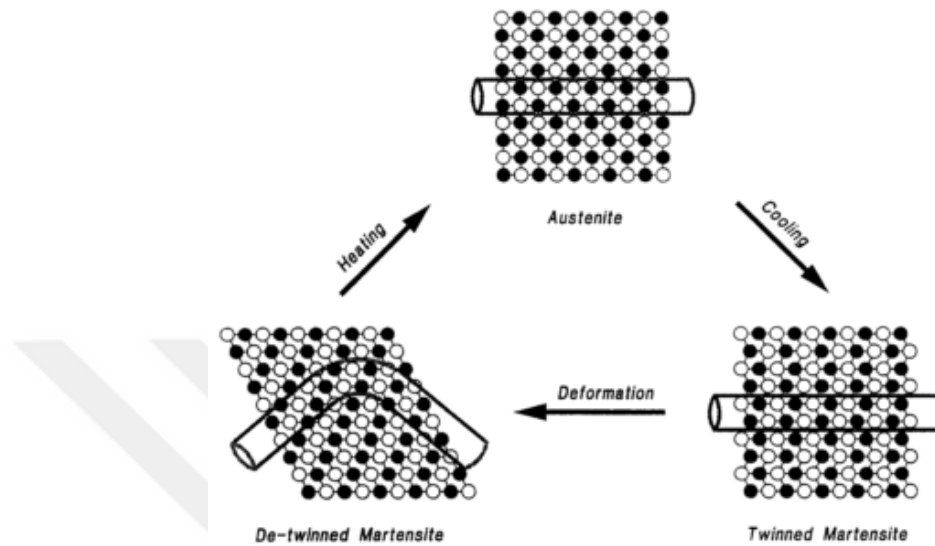
Figure 4. Depiction of shape memory effect [3]

In conventional metallic alloys, external stresses of higher magnitude than certain values, induce slip in the crystal lattice which then presents itself as permanent displacements and deformation. Shape memory alloys however, act contrary and after external stresses pass a known magnitude, a stress-induced transformation occurs. Alloy transits to martensite phase and behaves according to martensite mechanical properties. If the temperature is kept within an acceptable range (in which austenite exists) removing the external stress will result in a springback, instantaneous shift to austenite recovers the initial shape. Behavior of shape memory alloys in a stress-induced transformation then is called super-elasticity (SE) in which the alloy does not undergo a change of temperature, passing the martensite start temperature [3].

According to super-elasticity any deformation occurring before 100% transformation to martensite is fully recoverable. Permanent plastic deformation only happens in the fully

martensite region [3]. Conventionally this full transformation to martensite phase takes place around 8% strain which is demonstrated in Figure 5.
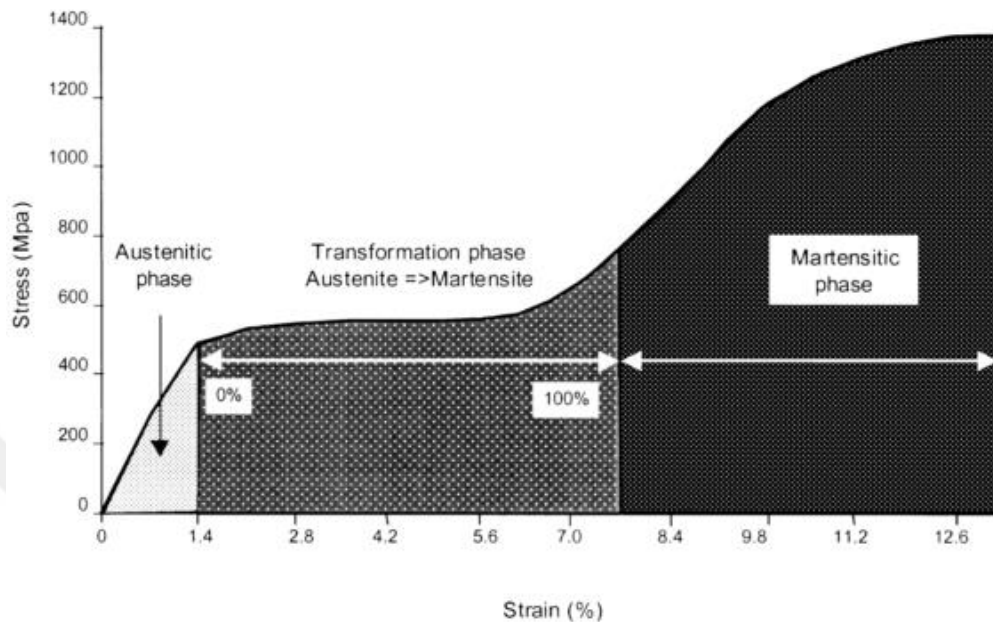
Figure 5. NiTi phase transformation according to increase in stress. the darkest part is permanent plastic deformation region [3]

1.3.   Effects of Heat Treatment

It is well understood that behavior of shape memory alloys like NiTi can be significantly altered via variation in their manufacturing and treatment [10]. Even slightest change in the chemical composition will invoke considerable differences in response [11]. Since the early decades of shape memory research, effects of heat treatment and cold work on transformation and super-elasticity behavior of SMAs have been investigated [11–13]. Heat treatment temperature and duration are capable of strongly influencing critical phase transformation temperatures between martensite and austenite phases [11]. It is known that cold work results in increase of strength in NiTi but reduces the recoverable strain values. This is due to appearance of new dislocations in the material [14]. On the other hand,

annealing restores shape memory effect while lowering material's strength. This is also explainable by dislocations being rearranged during heat treatment [14].

This makes investigation of annealing effects on behavior of SMAs of grave importance. Yeung et al, [11] propose annealing temperatures to be divided into three ranges: (1) solid solution treatment at high temperature 800–900 °C; (2) ageing treatment at medium temperature 400–550 °C; (3) ageing treatment at lower temperatures 200–400 °C. They also mention that applied cooling process (air-cooling, water quenching or furnace cooling) will also have numerous different effects on transformational behavior of the alloy [11]. In the following paragraphs, effects of heat treatment on one-way shape memory effect and super-elasticity of NiTi are presented, which will prove essential in different stages of this thesis.

In 1988 Yinong and McCormick [12] found that at minimum annealing temperature of around 550°C, the stress required for inducing a transformation to martensite phase has its minimum. They also observed that treating NiTi at about 600°C will result in higher stress induced strain. They gathered this information by conducting their experiments on near-equiatomic NiTi, annealed in temperatures between 397 and 927°C followed by air-cooling.

Miller and Lagoudas [10] investigated the effects of both annealing temperature and cold work percentage on transformation temperatures and latent transit heat. They subjected identical specimens to different percentages of cold work between 10 to 40% and parallel to that three annealing temperatures of 300, 400 and 500°C. Their experiments show that treatment in 500°C results in intermediator R phase in cooling process. 400°C results in the highest transition temperatures (both A_f and M_f). It can be roughly estimated that increase in annealing temperature increases the amount of transformation latent heat. Simultaneously higher rates of cold work decrease this value (Figure 6).
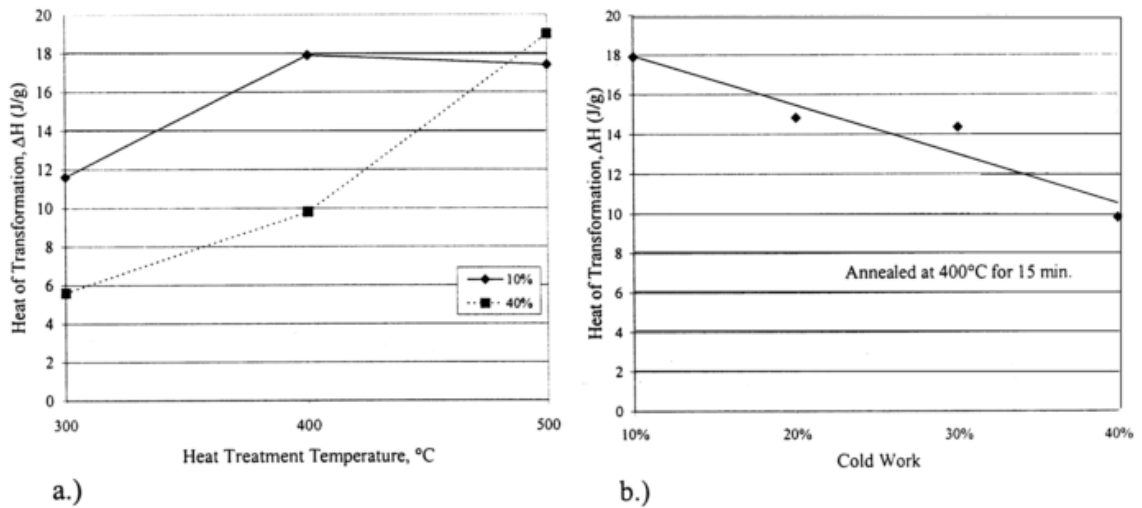
Figure 6. Effect of (a) annealing temperature and (b) cold work on latent heat of transformation

for NiTi specimens [9]
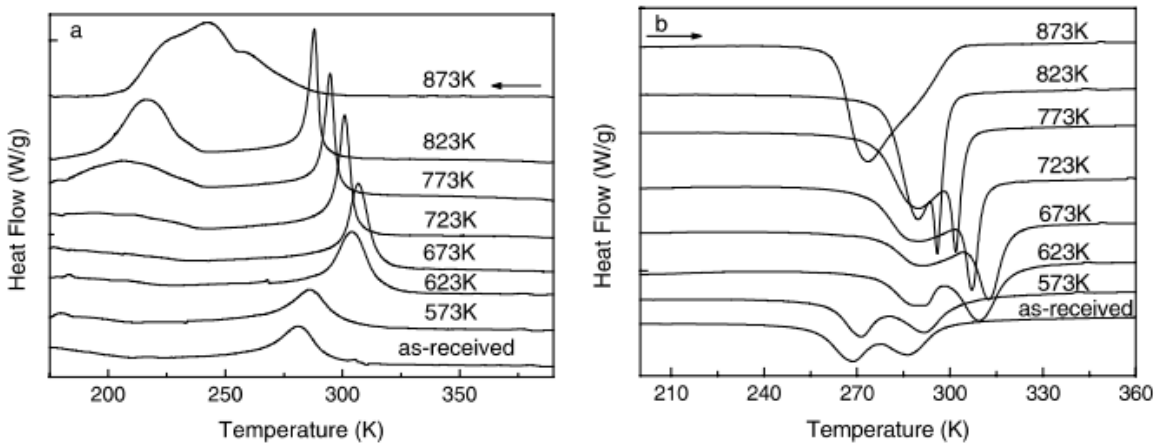
Figure 7. DSC graphs of a) cooling and b) heating for samples treated at different temperatures

[13]

In another study by Huang and Liu [13], different annealing temperatures between 300 to 700°C have been investigated, each for 30 minutes and followed by air cooling to room temperature. Each sample's transformation behavior then has been monitored via DSC. It shows that the sample annealed at 350°C possesses the highest transformation temperatures (Figure 7).

Simultaneously, this demonstrate that annealing above 550°C induces the demise of R-phase. One other finding of this research is effect of these annealing temperatures on

mechanical properties of NiTi. They conclude that increasing annealing temperature decreases the plateau stress.

Yeung and co-authors in an attempt to optimize treatment of NiTi alloy [11] experimented with higher annealing temperatures in duration of an hour and compared the result of solid solution treatment with and without aging process following matching with different cooling methods. It is discovered that aging combined with furnace-cooling or water-quenching produce the highest transformation temperatures (Figure 8).

Subsequently, while pointing at effectivity of cooling rate and time of heat treatment, they pronounce heat treatment temperature as the most crucial factor determining phase transformation temperatures.

Moreover, Mitwally and Farag [14] have discovered more about the effects of cold rolling coupled with annealing on mechanical and transformational properties of NiTi alloy. According to their publication, higher cold roll percentage results in higher recoverable strain value and fracture stress (Figure 9).
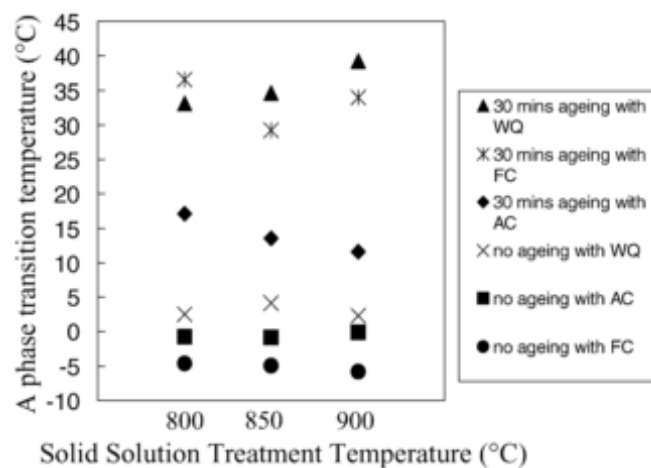
Figure 8. Austenite phase transformation temperature after 60 min treatment [11]
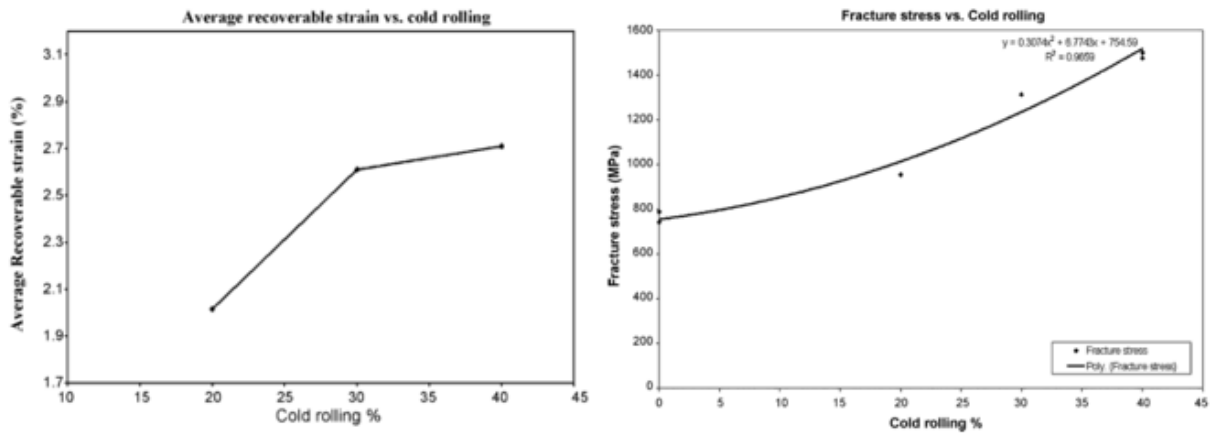
Figure 9. Recoverable strain (left) and fracture stress (right) as function of cold rolling [14]

In the same work, they have presented the effect of annealing temperature on hardness of the alloy. Accordingly, it is deduced that annealing at 500°C produces the lowest hardness value, which is lower than the as received properties (Figure 10).

Their research also touched on the superelasticity properties of the alloy and report that cold rolling deteriorates superelasticity of NiTi, but higher rolling percentages have higher superelasticity values in comparison to lower percentages. Similar to hardness results, they have reported that annealing at 500°C results in the lowest superelasticity value (Figure 11).
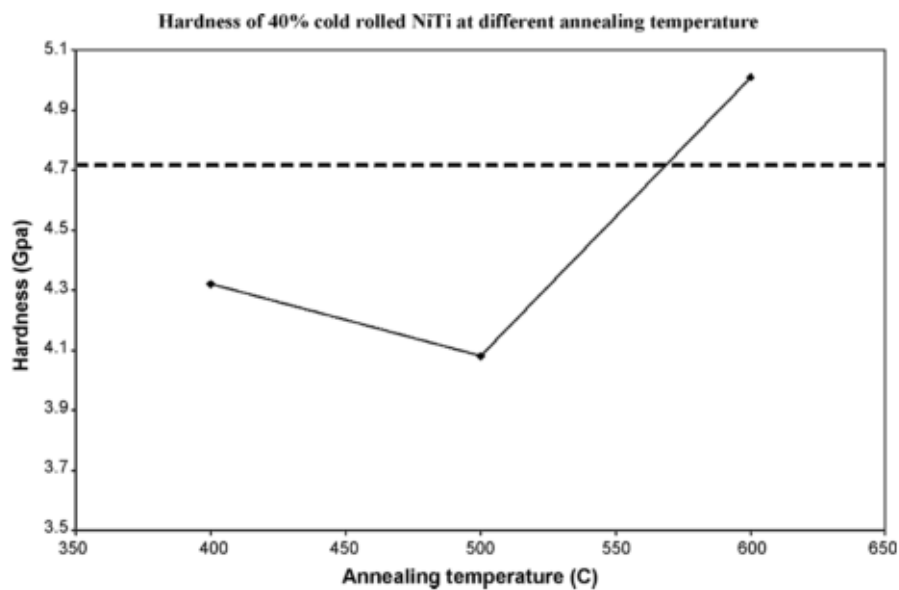
Figure 10. Hardness of 40% cold rolled NiTi annealed at different temperatures vs. annealing temperatures. The dashed line is for the as received material [14]
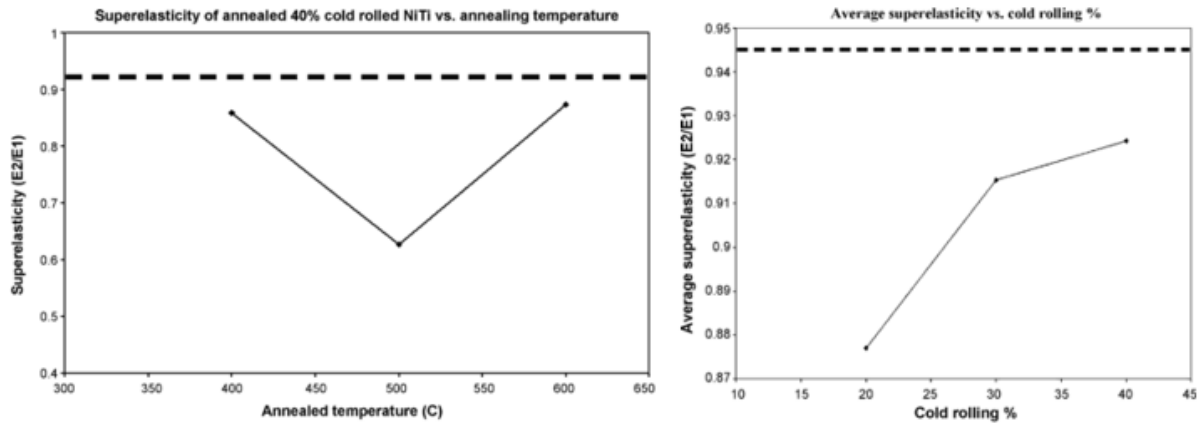
Figure 11. Average superelasticity values vs. annealing temperatures (left) and cold rolling percentage (right). The dashed line is for the as received material [14]

In the same work, it was also concluded that at 500°C recrystallization occurs and grain growth increases as the annealing temperature is increased which then presents itself as an increase in superelasticity and hardness.

Review of the previous research on effects of heat treatment on shape memory effect, establishes importance of working with different annealing temperatures and durations for achieving desirable shape memory behavior. It is also deducible, that annealing temperatures between 400º and 600ºC are the most repeated in numerous approaches.

1.4.   *Previous Work on SMA Actuation*

SMA properties, such as large force to mass ratio and increased stiffness at elevated temperatures make them an appropriate choice for actuators [15]. Using conventional motors as actuators requires several parts including gears and clutches to perform delicate and small displacements [16]. SMAs can be suitably utilized for micro-sized actuators which could be imputed to their structural and mechanical features such as their ability to be solely actuated via resistive heating [15]. These alloys are categorized as direct drive linear, being actuated while going through a phase transformation. This property eliminates the use of aforementioned excessive parts of conventional systems. At the same time the absence

12

frictional contact between dynamic elements, provides noiseless and lubrication free application. SMA powered actuators are also the most suitable option for clean room operations, since there is no dust spread during actuation [17]. Another advantage of these alloys against conventional actuator systems is their ability to be actuated via significantly lower voltages[17]. SMA embedded actuators are being introduced in medical, aeronautics and automotive industries, targeting simplified structures with reduced wear and corrosion minimizing costs of manufacturing and maintenance [18,19]. In this part, a chronologically review of the previous examples of actuator designs based on shape memory effect of these alloys is gathered.

One of the most conventional shapes of NiTi alloy available to actuator designers is NiTi wires which most commonly in industry are called as muscle wires. These manufactured wires are capable to contract to 5% when heated. Accordingly, many of the proposed designs in years have been focused on incorporating this type of wire deformation [20]. Simultaneously, it is possible to induce a desired shape to the austenite phase, utilizing the aforementioned annealing process. If kept in a die while annealing, wires will then possess a new memorized shape which would be recoverable when heated [21]. Basically, in an SMA embedded actuator transformation process from martensite to austenite is referred to as actuation.

Three basic types of actuation systems are known to be used for one-way SMAs: 1. One-way actuators 2. Biased actuators and 3. Antagonistic actuators [22] (Figure 12). In the late 1980s, Koji Ikuta and co-authors, proposed a comprehensive design for an active catheter utilizing more than one wire to actuate antagonistically. This proposition brought about a new way of utilizing SMA wires and empowering their position in competition to other conventional actuators [23]. A couple of years later, Bergamasco et al. [24] claim antagonistic configuration to serve as the beginning of SMA actuation systems. Coupled

13

with conventional control algorithms, SMA actuators can be trained to act similar to step-motors being called as multi-step SMA actuators [25]. This architecture can further realize the incorporation of SMA actuators in robotic systems.
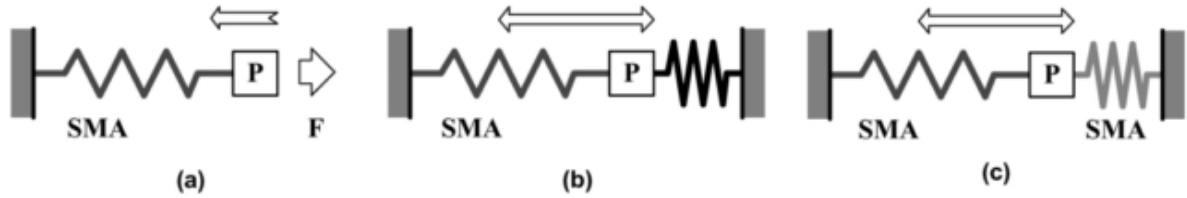
Figure 12. Types of actuator systems (a) One-way (b) biased and (c) antagonistic [22]

One of the main short-comings of SMA actuators is their limited strain [26]. Displacement in an SMA actuator is directly provided by mechanical strain during phase transformation. Actuator designers had to come up with different configurations to improve this crucial disadvantage of SMA actuators. In designs proposed by Ikuta [23] or Bergamasco [24] muscle effect of the wire is utilized while a major alteration is imposed to the form of the wire before application to improve displacement limit. They proposed wires to be used in coil spring form. In order to manufacture these coils, wires are wound and then annealed in a clamped packed constriction to receive the new shape as memorized [20]. Using spring form provides bigger displacement when actuated.
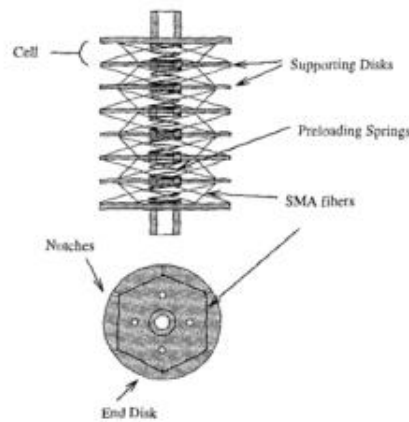
Figure 13. Grant and Hayward's actuator concept [26]

In an attempt to amplify displacement, Grant and Hayward [26] suggested a new design consisting of SMA wires woven around several supporting discs. In between discs, conventional preloaded springs are positioned. When actuated, SMA wires will compress the structure providing a bigger displacement (Figure 13).

Bergamasco, in his paper on shape memory alloy microactuators [24], concludes thermomechanical characterization and definition of geometry as two important steps in designing an SMA actuator. Thermomechanical characterization is in order a means of providing performance indices of the alloy. Performance index (PI), mechanical and chemical properties of alloys come to assist designers, in material selection [22].

In the late 90s, development of SMA actuators spread into many different fields. MEMS engineers, Kahn, Huff and Heuer proposed a novel micropump prototype utilizing antagonistic actuation of two SMA thin films [27], and a prototype incorporating a biased system, comprising of one SMA film complemented with a silicon spring design [28], and pronounce NiTi thin films a suitable choice for MEMS devices due to their considerable recovery forces.

Still incorporating contractile muscle wires many publications focused on expanding displacement of the actuation in the form of bending from a macroscopic point of view on the basis of binding a flexible wire to a contracting shape memory counterpart [29,30].

As mentioned, antagonistic actuator structure can be incorporated to make two-way SMA actuation by using one-way elements, since austenitic transformation of constrained NiTi exerts stress far greater than that needed to deform an identical NiTi in martensitic low temperature phase. Antagonistic flexural actuators are a proposed structure to utilize this agenda [31]. In a flexural actuator, SMA element deformation happens as bending, in contrast with muscle wires which contract. Inspired by nature and alive organisms, several

researchers have incorporated antagonistic flexural SMA actuators. Among those, micro-robot fishes are mentionable (Figure 14), in which micro biomimetic fins empowered by SMA actuators, provide propellant forces required for swimming in a gearless and noiseless manner [32]. Experiments show that these robots can swim in a direct trajectory and are capable of changing direction of movement.

Antagonistic flexural actuators also found their way into medical catheter and operational gear designs. Ho and Desai [15] proposed an antagonistic structure to be practiced in neurosurgical robotics, utilizing two bending NiTi wires, constraint to each other, providing a body joint, back and forth movement (Figure 15).
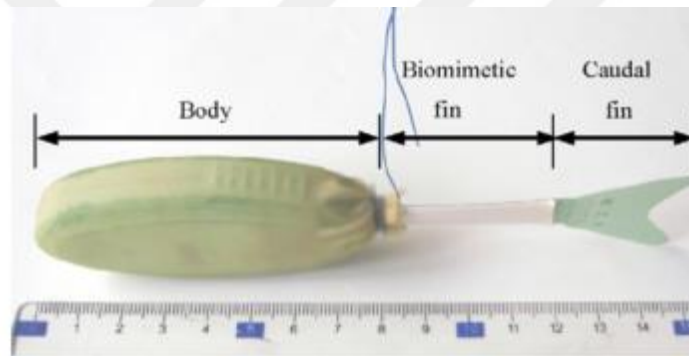
Figure 14. Micro-robot fish prototype courtesy of Wang, Hang, Li and Xiao [32]
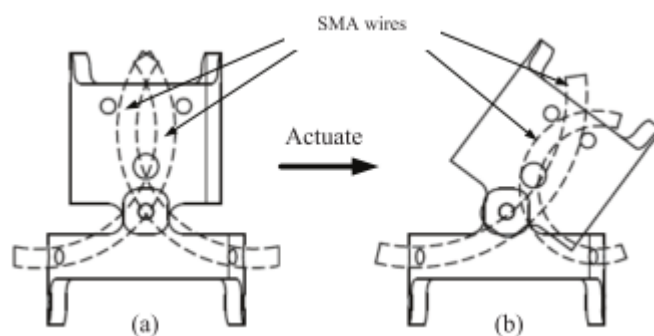
Figure 15. a. Stationary and, b. Actuated position of Ho and Desai robot design [15]

By the mid-2000s, SMA actuators had found their place in industry and their presence began to extend to every-day tools and structures. SMA actuated side mirrors are one of

utilizations of SMA actuators into consumer products after triumphant experience of their usage in medical and aviation industries [19].

One of arguably the most attractive approaches to SMA actuators is the incorporation of thin SMA films in folding smart structures (Figure 16). Nickle rich NiTi foil is designed and manufactured through negative photochemical etching process. Structures are designed and characterized such as near body temperature will activate the phase transformation in the form of an self-deployment, which makes them an innovative approach toward minimally invasive medical operations [33].
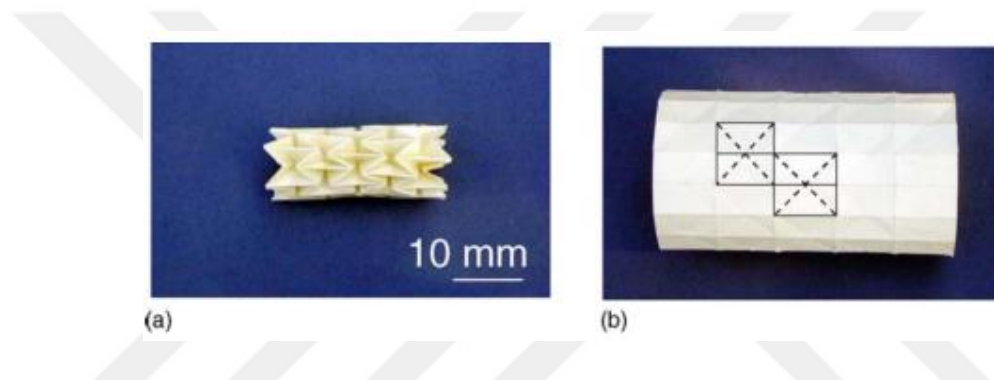
Figure 16. Photographs of a card model of the origami stent graft in its (a) fully folded, (b) deployed configuration [33]

Industrial presence of SMA actuators inhibited a fast-growing interest in catheter improvement. For decades, catheters have been broadly utilized in different medical procedures, improving precision and ease of operation at the same time, as well as minimizing diagnosis invasion and operation trauma [34]. Small size and clean operation of SMA actuators as well as accessibility of biocompatible NiTi alloy, drew attention of catheter designers to these materials.

Many proposed catheter related designs and researches have been conducted at Japan in the 90s. Haga, Tanahashi and Esashi [35] proposed a jointed catheter structure with a small diameter of 2mm, applying actuation of three coiled SMA wires at each joint to achieve desirable maneuverability, and characterizing Joules heating by electrical current

17

thoroughly. Presenting bending characteristics of the catheter against electrical current enables manufacturers and users for further path planning requirements when it comes to utilizing such device [35]. They were focusing on kidney operation and have successful modeled operations on representative models of such organ. Making their case stronger they also present two non-jointed structures called endoskeletal and exoskeletal structures depending on their structure, broadening the area of application their design would cover. Consequently, the ensemble proposed batch assembly method using nickel electroplating to exert total control over performance of smart material after manufacturing [36]. Batch forming by photo-fabrication process makes intricate patterns achievable [37].

Further research on catheters introduced sensors into these devices. Presence of sensor such as tactile sensors [38] enables the system to be aware of its surrounding. Covering tip of a catheter with mentioned sensor will prohibit further actuation at the moment of contact, making them adaptable for intricate operations and intravascular cerebral approaches.

Table 1. SMA actuator iteration and characterizations done for tubular actuator [40]

Picture	No.	Max Force[a] (Austenite)	Force Ratio (Aus/Mart)	Stiffness Ratio (Austenite)
	1	1790 mN	1.9	.64
	2	2000 mN	2.4	.87
	3	330 mN	2.5	.94

[a]Measured at 300 μm

One structure popularly utilized in catheter actuator design is tubular SMA units, etched into different formations [39]. It is argued that tubular laser machining of NiTi provides suitable structure for catheters and other similar apparatus and manipulation of the machining fabrication of the actuator can be utilized for improving specific properties of the

system as listed in Table 1. Maximum exerted force is one of the properties drastically depending on architecture of the actuator [40].

In 2007, building upon propositions of Icardi [29] and Wang and Shahinpoor [30], Veermani et al. [41] developed a fully functioning active catheter using only one central NiTi tendon. They further depict high accuracy of their system even for high bending angles of +90 degrees. They also introduced the use of optical 3D tracking systems to perform as a positioning sensor while testing the catheter.

Building upon the same concept, Crews and Buckner [42] increased the number of long thin SMA wires to four, positioning them around the center-line of the catheter, resulting in bending maneuverability in four directions. This approach enables the device to be fully controlled while bending and resetting, being able to reach every point in the field without the need to spin the body of catheter.

As a novel actuation strategy, Ayvali et al. [43] introduced flexural antagonistic actuators into catheter like structures, via incorporation of two antagonistic NiTi wire actuators, shape memorized as arcs in steerable needle/cannula. It is then claimed that this design will enable placement of flexural actuators along the cannula, while each is actuated disregarding others. As well as shape memory effect, superelastic behavior of NiTi shape memory alloys has also found their way into medical industries. Their unique shape recovery properties enhance minimal access surgery procedures, by actualizing implantable devices [44].

Parallel to innovational discussion and commotion surrounding shape memory alloy actuators the matter of characterization and control of such devices rose to attract attention of mechatronics and control engineers. The non-linear behavior of such actuators and complications regarding cooling of these system were among the most problematic aspects

19

of this practice [45]. As one of the early investigations tackling cooling of these devices, Reynaerts and van Brussel [45] suggest forced liquid cooling as a solution to linearize hysteresis of SMA actuation in order to obtain higher accuracy. This investigation aims to contribute insights into the development of an antagonistically actuated active joint as an expansion to the present body of knowledge.

CHAPTER II

2. PROBLEM DEFINITION

In numerous medical and industrial cases of SMA actuators, a recurring trait in design is the systemic approach to distribute actuation of the entirety of the system into discrete localized links [15,35,43]. Distribution of actuation enables designers to achieve more precise movements in the system. In case of catheters, a jointed structure provides maneuverability within intricate pathways. Moreover, having several links will reduce the cost of maintenance and repair in any system. As a wider approach, this study is focusing on design and development of a capable actuator unit, to be installable in a number of robotic system, medical or industrial. As mentioned in the introduction, NiTi shape memory alloys are satisfyingly biocompatible [34], making them a suitable option to make sure the presented actuator unit has the capacity of playing a role in medical instrumentation. Also, breaking down a system into a segmented structure eliminates the need for an elaborate single component actuation system which provide more than one degrees of freedom. In the presence of this requirement, a modular, segmented system can incorporate a comprising architecture that in return provides such maneuverability. Having these points in mind, this research confined the requirements of such unit in providing a single degree of freedom in displacement, which is substitutable with conventional motorized robotic joints. The resemblance of these units to organic joints compelled the researcher toward coining these actuator units as active joints. The following body of work will present the development of an active joint, empowered by shape memory alloys, providing joint-like displacement described as bending.

CHAPTER III

3. CONCEPTUAL DESIGN

This section has been divided into two parts; firstly, dimensional and required physical criteria of the joint will be established and secondly, systematic concepts designated to satisfy the actuation and motion objectives will be presented. Limiting a prototyping project in size and requirements will improve quantitative and experimental study of each concept at hand.

3.1. Operational Criteria

Provided that this so-called joint is to be incorporated in multiple applications including medical tools, the cross-sectional area of the device is of utter importance. Narrow body cavities and canals permit objects of definitive circumference passing through. To be incorporated in an apparatus, a typical joint is required to possess these criteria:

1. Outside diameter around 4mm.

2. Circular cross-section to provide all-around performance.

3. Bending and straightening on command.

4. Bending capability up to 90º.

Possible conceptual designs have been put forward to satisfy these objectives. Limitations in design objectives were taken as a guide line, confining proposals to a cylindrical body form for the joint, consisting of a 10mm length and cross-sectional diameter of 4mm. Forthcoming proposals had this structure in common.

3.2.   *Conceptual Proposals*

3.2.1. Proposal I: Passive resetting via flat spring

First proposal comprised of one shape memory and one flat spring, confined between a pair of couplings at both ends to hold them structurally together. Principally, SMA wire would actuate when heated and transform to austenite phase, imposing bending motion. When cooled down, simultaneous to its transformation to martensite phase and decrease in strength, the flat spring would provide enough stress to bring back the entire structure to initial position or in other terms, to reset the joint. Two different designs for this concept were brought forward:

1. Fixing both elements in the same surface as the surface of SMA bending, which would result in different radius of curvature in bent position for both elements (Figure 17). When bent, this structure is prone to a systematic disadvantage. At a given bending angle, both elements will share one surface of bending while having different distances to the center of curvature. This configuration is only suitably implemented if either the flat spring is compressible or the SMA wire is stretchable, or if the joint provides enough space for flat spring to acquire a much smaller radius of curvature, which will translate into limited space for further equipment passing the joint.

2. Fixing them on a surface perpendicular to the surface of SMA bending, which would result in equal radius of curvatures in bent position for both elements (Figure 18).
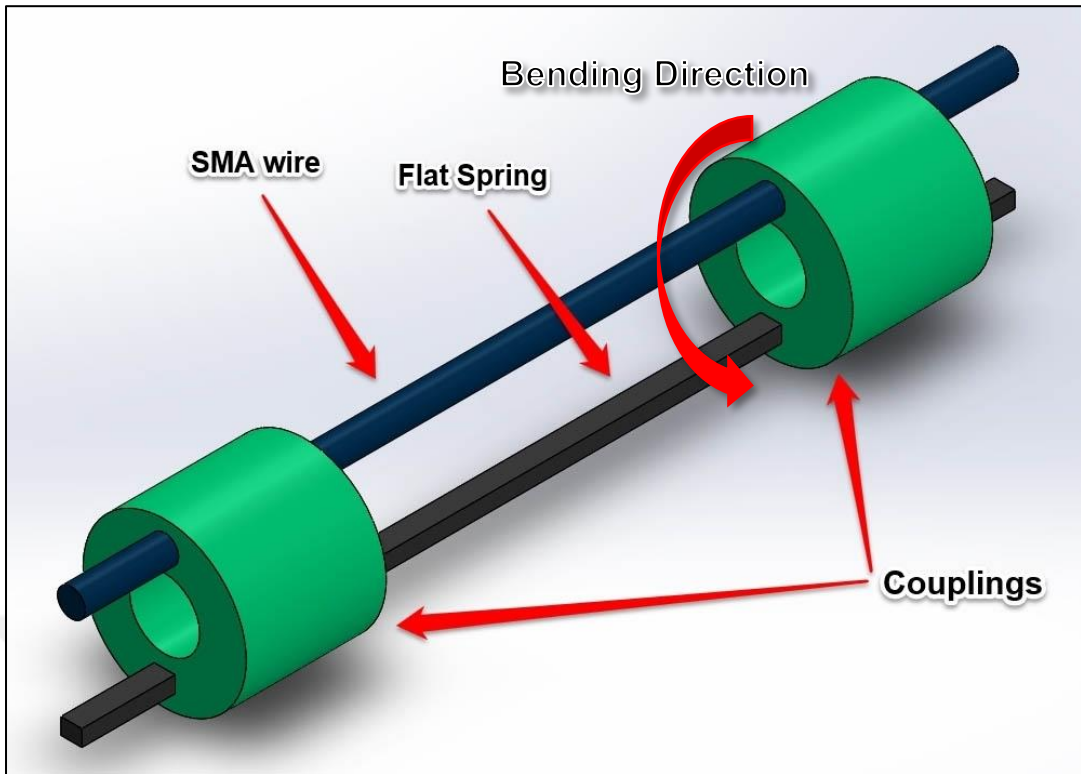
Figure 17. Three-dimensional presentation of concept I-1
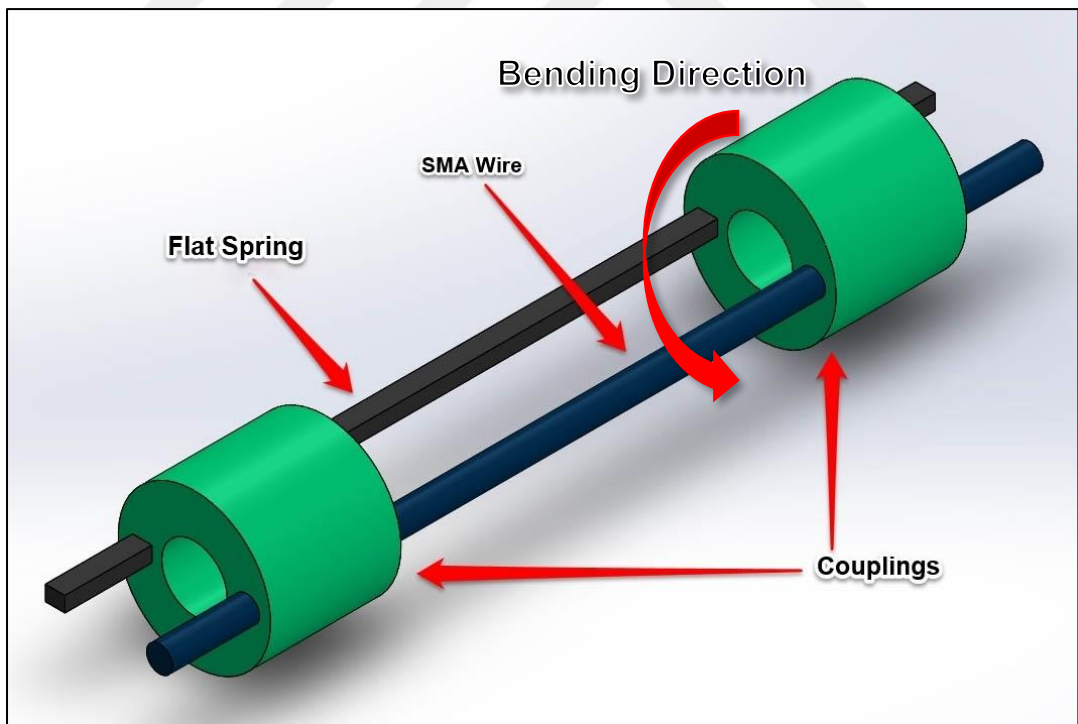
Figure 18. Three-dimensional presentation of concept I-2

This second architecture is prone to undesired torsional moments, resulting in the twisting of the joint. This unwanted reaction will in turn limit the bending capacity of the joint and uncontrollable force excursion into multiple undesired directions.

3.2.2. Proposal II: Passive Resetting via coil spring

This concept consists of a coil spring encompassing the joint at the bendable area, substituting the flat spring, providing a uniform distribution of moments exerted by different elements while providing larger workable areas within the joint for future usage (Figure 19). Coil spring will act as the resetting element when the bending element (SMA wire) is cooled down. The same as flat spring, coil spring provides an ever-present dynamic stress, propelling the joint back into the straight initial position.
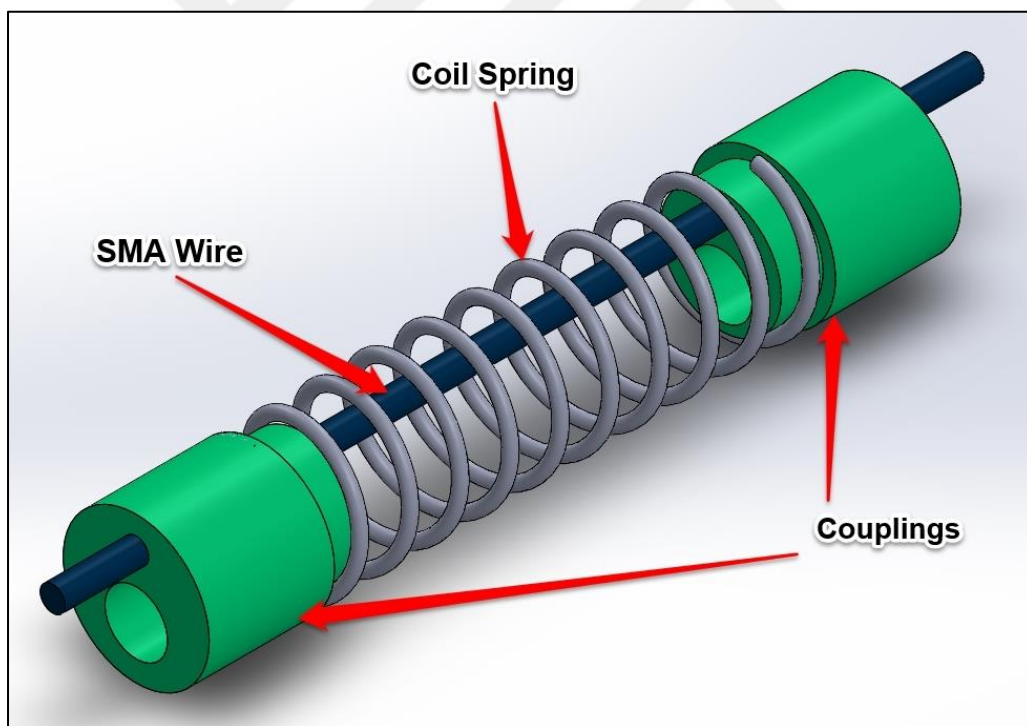
Figure 19. Three-dimensional presentation of concept II

Positioning of the SMA wire and uniform surrounding of the coil spring provides a symmetrical structure which is satisfactory in case of eliminating undesired moment or stress. Coil spring is supposed to provide sufficient stress to bend back martensitic NiTi back

into initial form and submissive resistance against stress provided by the austenitic NiTi. Plausibility of this architecture is to be further investigated in coming sections.

Passive resetting is estimated to impose the prototype to imperfections in controllability. In addition, it is observed that exerted stress by beam or coil springs only depend upon their deformation (strain), and provide identical resistance in both bending and resetting stages of actuation. Having these two principal characteristics of passive resetting method, incorporation of active resetting might solve possible short-comings of the aforementioned concepts. Hence two forthcoming concepts are efforts to introduce active resetting into the same joint.
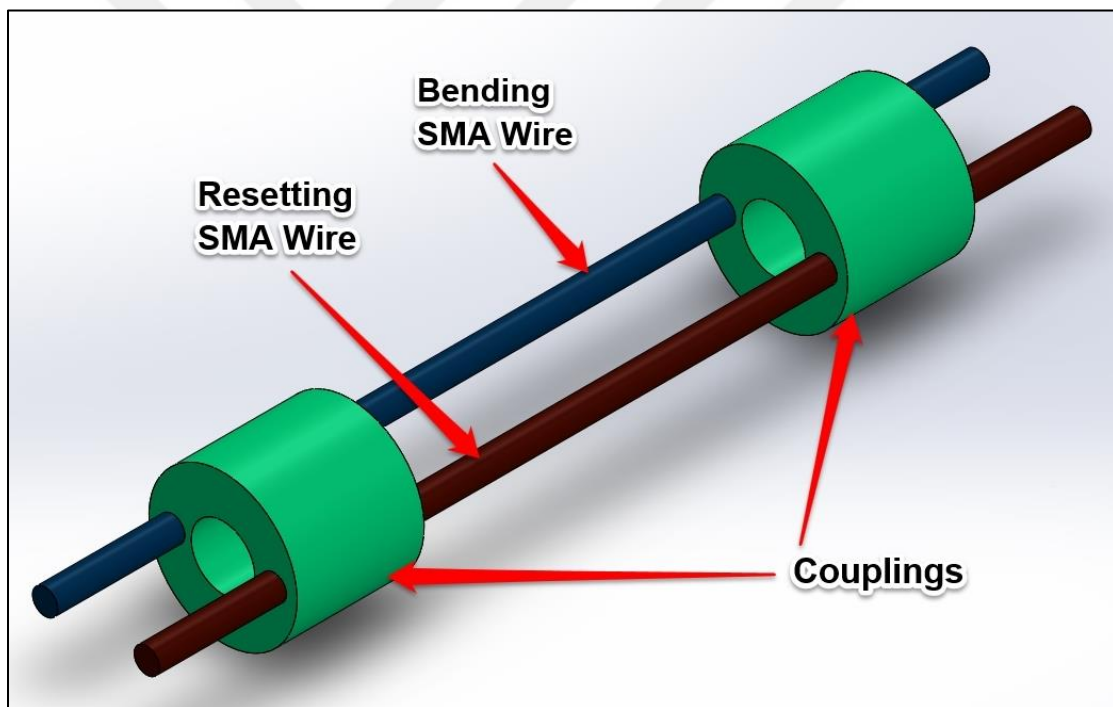
Figure 20. Three-dimensional presentation of concept III

3.2.3. Proposal III: Active resetting via antagonistic SMA wire

This proposed structure comprises of two SMA with two different austenite macroscopic shapes, one bent and the other straight, confined between two cylindrical couplings (Figure 20). When heated, bending wire will transform to austenite phase, bending to its memorized

26

shape and in return desirably bend the entire joint. Resetting wire will transform to straight austenite shape when triggered, providing moment to straighten the joint as a united system.

Positioning wires in this manner seems like the only likely option, but it will result in asymmetry of forces provided by SMA wires and produce a structure prone to twists and imperfect translation of moments between two wires. Lack of mechanical connection between the two wires also magnifies this undesired effect.
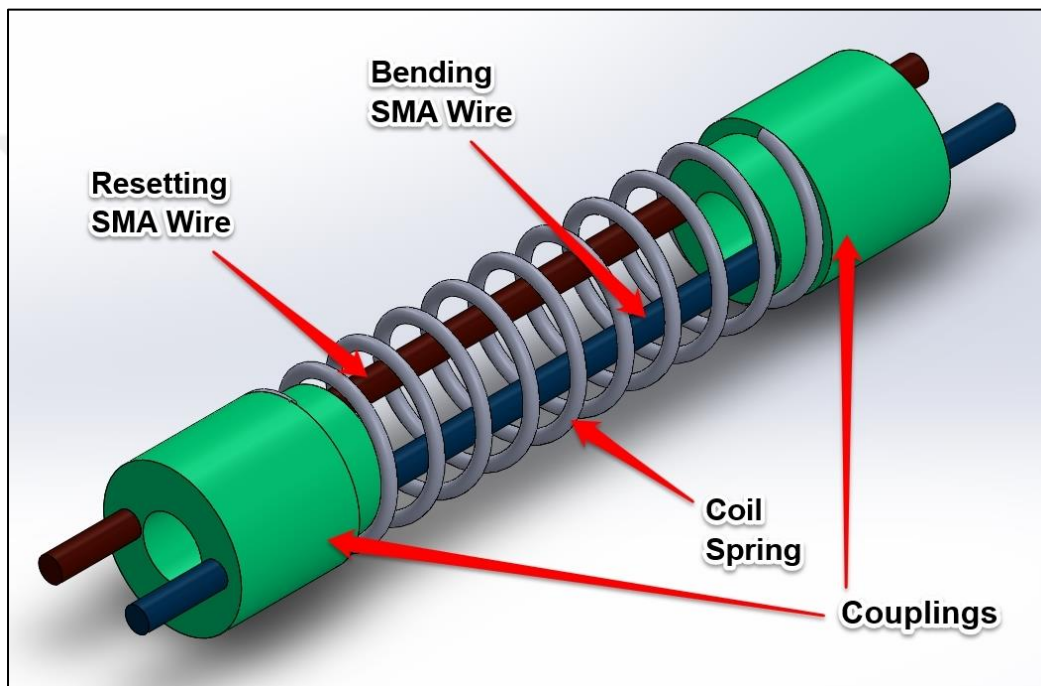
Figure 21. Three-dimensional presentation of concept IV

3.2.4. Proposal IV: Active resetting via resetting SMA wire in presence of encompassing coil spring

To improve short-comings of the previous proposal, the same envelope coil spring as the second proposal is introduced to the system (Figure 21). Two SMA wires will work in an antagonistic manner. Coil spring will reduce unwanted deformations and twist in the structure. To use the spring for solving lack of mechanical connection between two actuating SMA wires, wires are positioned close to the coil spring.
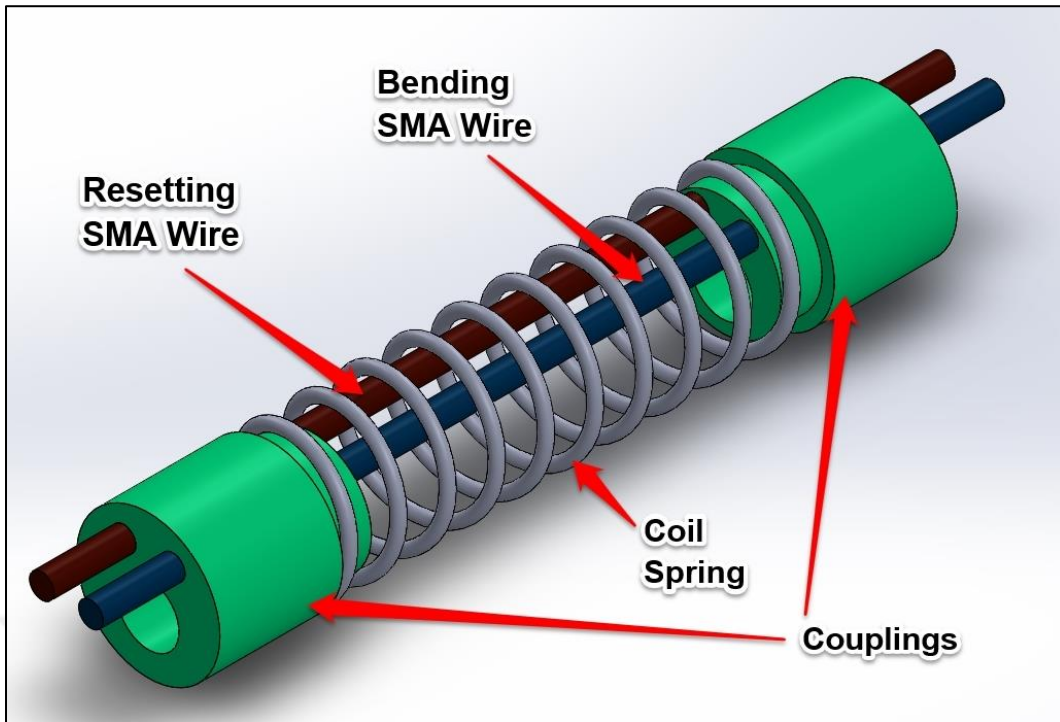
Figure 22. Three-dimensional presentation of revised concept IV

To further eliminate the twist and asymmetry in dynamic structure of the joint positioning plane of the wires will be moved further near to each other (Figure 22). This will introduce a form of attachment which will act as a bridge to transfer moments between the two wires.

3.3. Concept Selection

Among these four proposed structures and six designs, three are based on passive resetting of the joint.

Proposal I – 1st design introduces geometrical paradoxes. Sharing one bending angle between the two wires is impossible because of their different offset from the center of curvature. This will result in inconsistent bending angles and extra resistance.

28

2nd design introduces twist, in a manner that SMA wire is not able to bend the flat spring identical to its own curvature. On another issue, experimental trials of this concept propose impossibility for resetting back to straight position. Deformation of a bent metallic rod, requires a constant moment, given the material does not go through phase transformation while it is being reset. A flat spring, acts similar to a flat spring, exerting moments dependent on its deflection from the initial position, a presentation of the Hooke's law. Near the fully straight position, flat spring's exerted stress diminishes, which is interpreted into inability of flat spring effect to bend the SMA wire back to reclaim joint straight position.

Proposal II – Substitution of flat spring with coil spring eliminates the twist effect and balances dynamics of the joint. SMA can be positioned on mirror plane of the coupling which produces a symmetrical structure. On the other hand, coil spring is also bound to Hooke's law, linking its provided stress to its deformation. Similarly, this structure also cannot provide enough stress near straight position. Experiments on the prototype also prove this estimation in observations.

Proposal III - Structural identicality of stresses exerted by the two antagonistic wires can be experimentally proven. Phase transformation will diminish strength of resisting wire in each part of actuation. Drastically asymmetrical architecture of this proposal deteriorates its actuation behavior. This structure (like proposal I 2nd design) is prone to twist and imbalanced dynamics. Therefore, this design is not satisfactory as a working joint.

Proposal IV – Presence of coil spring encircling the joint tends to balance dynamical behavior of the joint. Moreover, it is experimentally argued that incorporation of a damping element such as spring in an antagonistic actuator will enhance tracking and settling time when installed in a control algorithm [46]. As an improvement, it was prototypically proven that close placement of actuation elements help with cancelling of the asymmetry of dynamics in the system.

This last design, when prototyped and tested, provided convincing initial behavioral results which placed it to the top of the list and absorbed the focus to further. The upcoming sections will provide further detail throughout development of this concept toward a fully functioning joint.

CHAPTER IV

4. EXPERIMENTAL PROCEDURE

After determining a concept as the guideline, a development plan is followed. Experimental efforts, heavily intertwined with this development plans are implemented. The essential elements in the joint are the two SMA wires, responsible for actuation. For joint development, characterization of individual SMA wires is of great importance. In addition, when assembled, performance of the joint in its entirety is put to experiment. Characterization of SMA wires comprises of determining the effect of process parameters on the functional properties.

4.1.   Heat treatment and Annealing of NiTi wires

The SMA material used in this work was equi-atomic NiTi wire. Since it is known that thermomechanical behavior of NiTi alloys change intensely when exposed to different heat treatment regimens [6,47,48], characterization of this material preceded other steps. Previously, annealing in a temperature range of 300°C to 600° and at durations up to an hour have been frequently investigated, presenting a suitable range and containing optimal points for different functional criteria [10,13,14]. Accordingly, a range of different heat-treatment parameters were set to experimentally determine the supplied material behavior.

At the same time, fixtures were designed to form wires in desired shapes in a condition reducing the possibility of oxidation. Plates were then housed inside steel encasement (Figure 23).

Figure 23. Picture of forming fixtures and their casing

Desired austenite phase shape of the wires depends on the desired outcome of the joint. As a goal, a bending up to 90 degrees has been targeted. Previous investigations on NiTi prove its ability to recover 8% strain after unloading and heating [7]. 8% strain while bending, in a wire of 0.6mm diameter with the arc length of neutral line (Ln) constant at 10mm, is translated as 140° of bending (Figure 24).
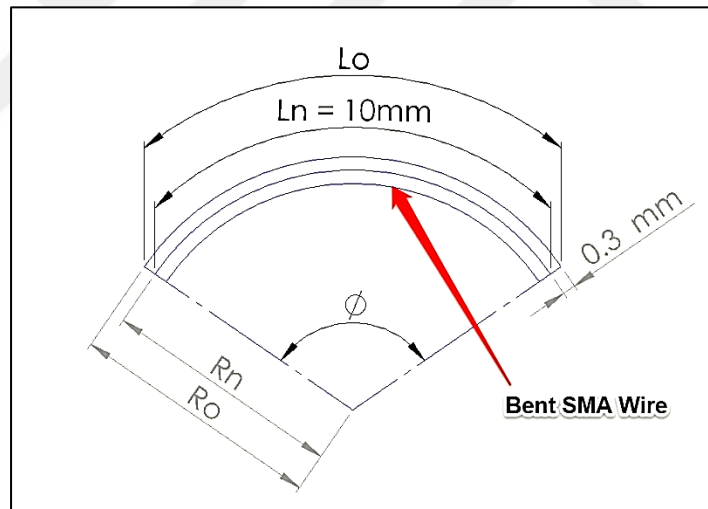
Figure 24. Schematic presentation of arc lengths and radia of curvature

Accordingly, different fixtures for different bending angles up to 140° were designed and manufactured to further investigate their behavior in the coming stages. NiTi wire was then cut and fixed into fixtures and sealed. Then, it was placed in a pre-heated oven at the set temperature for the set time. Consequently, the fixture was quenched in water to finish the treatment procedure. Afterwards, encasement is opened and samples were taken out for following experiments.

4.2.   Experimental procedures and setups for single wire characterizations

4.2.1. Actuation setup

After heat-treatment, wires possess a memorized shape. It is important to quantitatively observe their phase transformational performance. Per the fixture shape, wires will actuate after reaching a certain temperature (A_f).

To record the bending, a setup structure is then designed to confine the movements involved in this deformation, such that only one degree of freedom is remained and can simply be recorded. Fixing one end of the wire at a pivoting point and placing the other on a pivoted slider, will translate bending into uniaxial displacement of the slider (Figure 25). Recording either rotation of each pivot or displacement of the slider can then provide the observer with sufficient data to determine the bending angle of the wire. If needed, the linear displacement of slider can be recorded via a potentiometer or linear variable differential transformer (LVDT) sensor, whereas the rotation of each pivot is observable using an optical encoder.
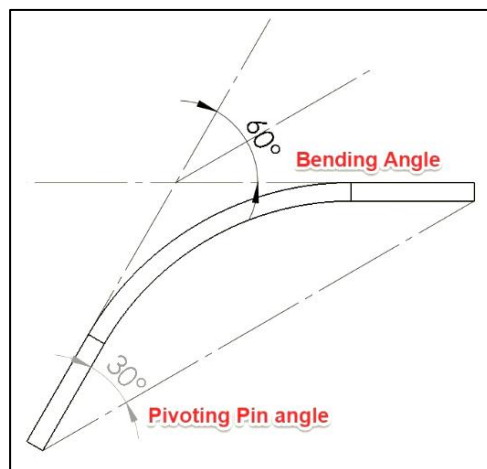
Figure 25. Depiction of bending angle and relative angle of each end read by encoder.

A setup is designed and manufactured (Figure 26) in which the rotation of stationary pivoting pin is connected to an encoder. This design is capable of recording its rotation which equates half of the size of bending angle of the wire if the bending angle is defined as the angle at the collision of tangent lines at two ends (Figure 25). If preferred, a hanger is allocated on the slider to connect it to a LVDT.

This setup facilitates observation of the phase transformation per rising temperature (readable by a thermocouple set attached) to determine austenite start and finish temperatures. Using a pulley and weight attached to the hanger will provide a setup capable of recording transformation performance in presence of dead weight. Subsequently, substitution of pulley and weight system with a spring will provide observation of the effects of dynamic loading on the wire (Figure 26-27).

Data acquired by encoder, LVDT and thermocouples are recorded and analyzed by custom LabView programs. Cyclic actuation programs were designed in order to provide a variety of performance scenarios based on time and temperature. A similar setup with fixed and movable pivots is used to characterize the behavior of the joint.

4.2.2. Force setup

SMAs exert forces during recovery to their austenite shape [27]. This specific force is the propeller of the actuator. Hence, it is vital to measure and control this load which is in correlation with temperature. A simple fixture is then designed to connect one end of the wire to a cantilever load-cell while the other end is fixed. The connection is perpendicular to both the wire and the load cell, making it possible for measurement. By having this data, the bending moment of the wire can be calculated. Temperature of the wire is monitored via thermocouples while the wire is undergoing actuation (Figure 28).
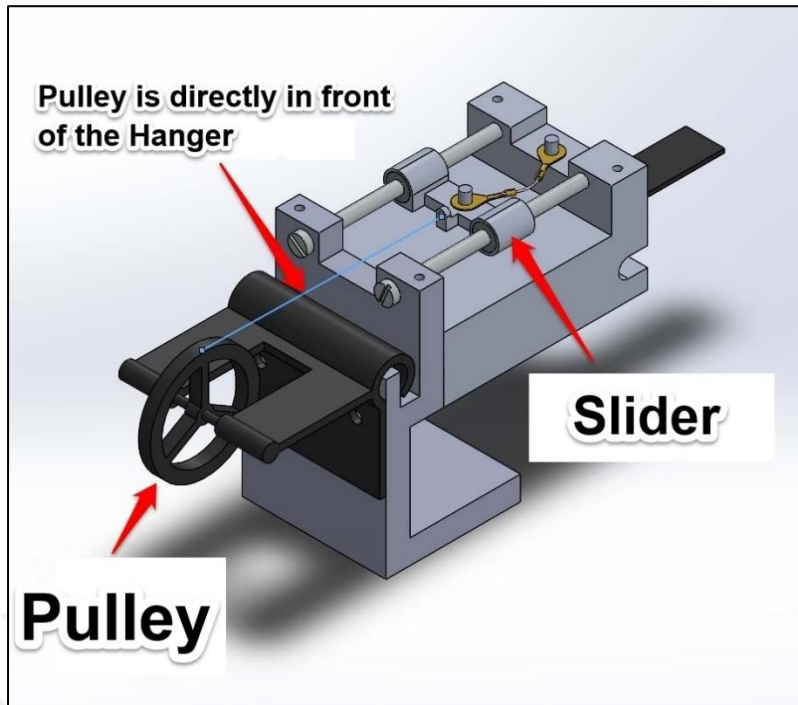
Figure 26. Three-dimensional depiction of the experimental setup.
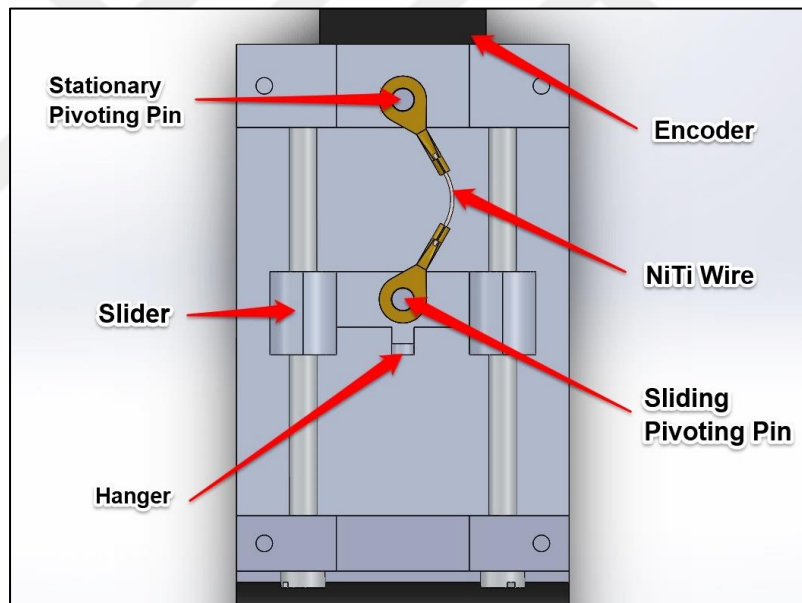
Figure 27. Top view of the experimental setup showing different components.
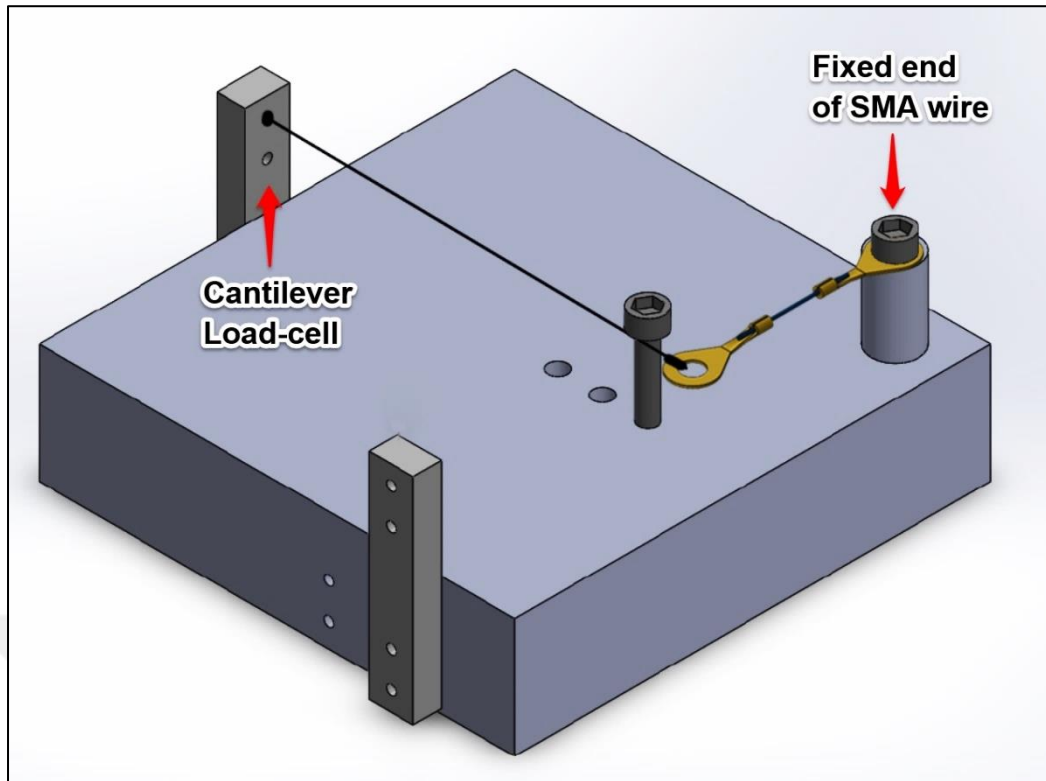
Figure 28. Three-dimensional depiction of cantilever fixture for SMA force measurements.

Figure 29. Picture of the DSC machine in the laboratory

4.2.3. Differential scanning calorimetry (DSC)

A very precise method for determining transformation temperatures of a shape memory specimen is differential scanning calorimetry, by which the heat flow inward and outward of a small sample while heating and cooling is measured according to temperature change. Inconsistent changes in the heat flow determine the phase transformation temperatures. As seen in Figure 29, a DSC machine has been used to determine these values at zero external stress [49].

4.3.   Experimental procedure and setup specific to joint performance test

In this case, a similar actuation setup is designed, comprising of a slider, fixed pivoting pin and an encoder. When project had reached this point, a sliding system with lower friction constant had been purchased and implemented in this design for further enhancing frictionless displacement of the sliding end of the joint. In order to better balance actuation of the joint, its plane of bending was changed into a vertical plane (Figure 30).
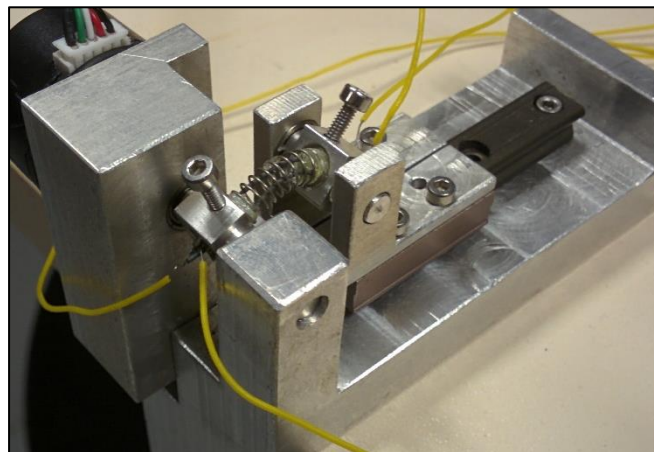
Figure 30. Picture of the cyclic behavior test setup while actuating an installed joint.

CHAPTER V

5. EFFECT OF HEAT TREATMENT

Previous investigations in this area which has been briefly presented in the introduction provides a comprehensive guideline for researchers developing SMA actuators. Most investigations have focused on the effects of the annealing method which has been introduced in the experimental procedure section [12–14]. Annealing temperatures between 300 and 1000°C have been investigated [11,12] and for actuation purposes a temperature range between 400 and 600ºC is advised [14]. Samples treated in these temperatures are less prone to inconsistent heat flow peaks and presence of R phase [13].

Similarly, effects of annealing differ if annealing temperature is altered. Consequently, researches have been showing different outcomes according to different annealing temperatures and a range between 15 to 90 minutes [8,11,47,50] has been most commonly applied.

5.1.   Investigation of transformation temperatures

Accordingly, a respective annealing table has been improvised which included three different annealing temperatures between 400º and 600ºC and two annealing durations 30 and 90 min, in order to broadly characterize the shape memory alloy. Then thermal behavior of the samples has been identified using differential scanning calorimetry to acquire their transformation temperatures (Table 2).

Findings are in compliance with previous literature [11] and present a repeatable trend. Figure 31 depicts this trend in which Austenite start temperature (A_s) increases with the increase of annealing temperature but samples treated at 500ºC tend to have relatively lower

Austenite finish temperatures (A_f). In both durations, the 500ºC produces the smallest gap between Austenite start and finish temperatures (sharpest peak).

Table 2. Transformational temperatures acquired by each different heat treatment condition

		Annealing Duration	
		30 minutes	90 minutes
Annealing Temperature	400ºC	A_s= 38ºC, A_f= 54ºC	A_s= 45ºC, A_f= 61ºC
	500 ºC	A_s= 43ºC, A_f= 56ºC	A_s= 46ºC, A_f= 59ºC
	600 ºC	A_s= 49ºC, A_f= 63ºC	A_s= 54ºC, A_f= 67ºC
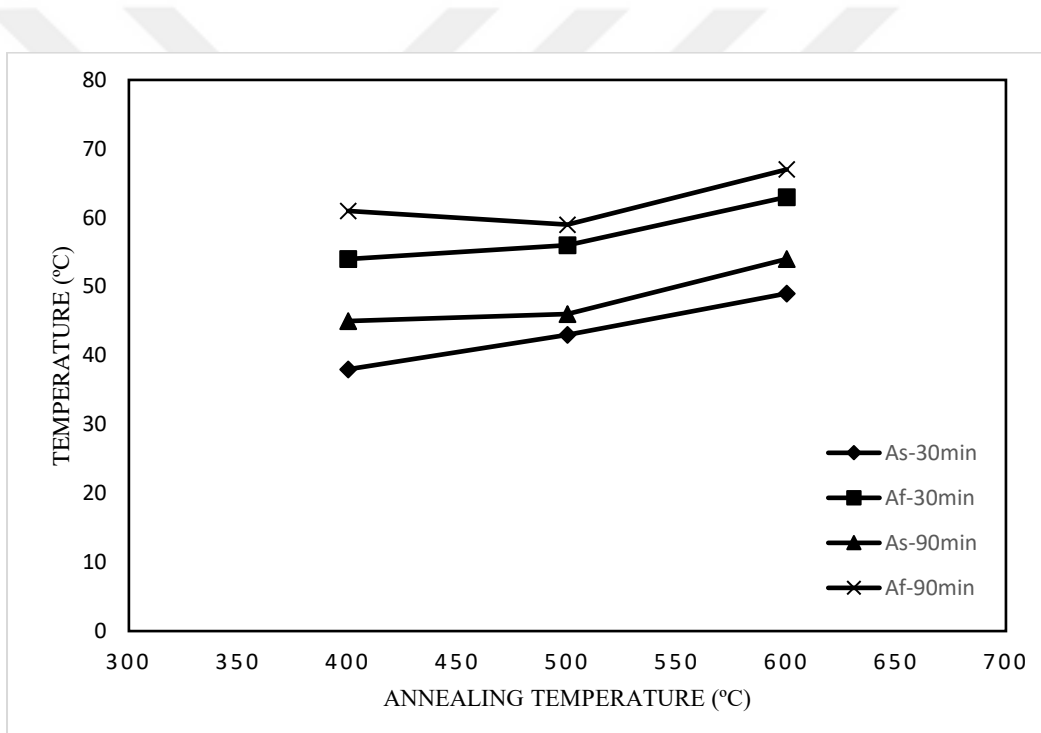
Figure 31. Transformational temperature against annealing temperature. Two different durations of 30 and 90 min are presented in this figure.

Smaller gap in between austenite start and finish means sharper and faster actuation capability for the joint, which makes treating at 500ºC a preferable procedure. On the other hand, decreasing transformation temperature values will limit the need for reaching higher temperatures and electrical current. This in turn enhances durability of the system and reduce

energy consumption. Accordingly treating the alloy for 90 minutes is proved undesirable. It is obvious that prolonging the annealing process should not be pursued.
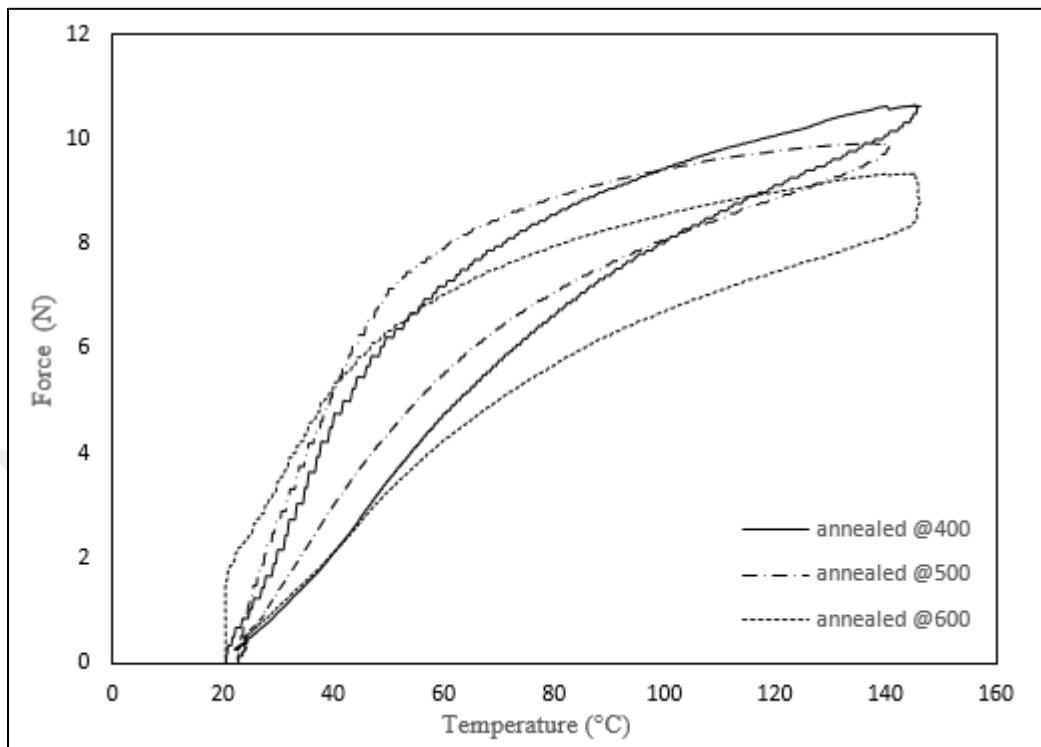
Figure 32. Force output of samples treated at different temperatures.

5.2. Investigation of force output value

Next the samples were tested in the load-cell setup to investigate their force output at forced constraint condition. Figure 32 presents the results related to samples treated for 30 min at different annealing temperatures. It can be deduced from the graph that the highest actuation force is obtained after annealing at the lowest annealing temperature. This observation is in line with a previous study [8] where higher annealing temperatures led to decreased transformation stress levels. In another study by Mitwally and Farag [14] annealing at a temperature of 600ºC revealed a surprising increase in the hardness as compared to reductions seen at 400 and 550ºC. In another research published by Yinong Liu [12] it is presented that increasing the annealing temperature decreases the stress value for

40

stress-induced martensite which is a similar conditional experiment as performed load-cell experiment. Constrained NiTi wires in this setup provide the stress which will constantly push forward their transformational temperatures due to stress induced martensite effect and simulate Liu and McCormick's experiment [12].

This phenomenon enables the sample treated at 500ºC to provide higher force value at temperatures between 40ºC and 80ºC. It has been established that Austenite transformation temperatures for these samples are between 38º and 67ºC. Accordingly, it can be deduced that a sample treated at 50ºC can be more influential in actuator design. Its lower force output at temperatures below 40ºC in comparison to other two samples, is translated as lower strength at these temperatures (majorly martensite phase). Having the antagonistic structure of the joint in mind, lower strength at martensite phase and higher force output at austenite transformation temperatures makes this sample the most satisfying option among others. Figure 33 present a sample for DSC test result.
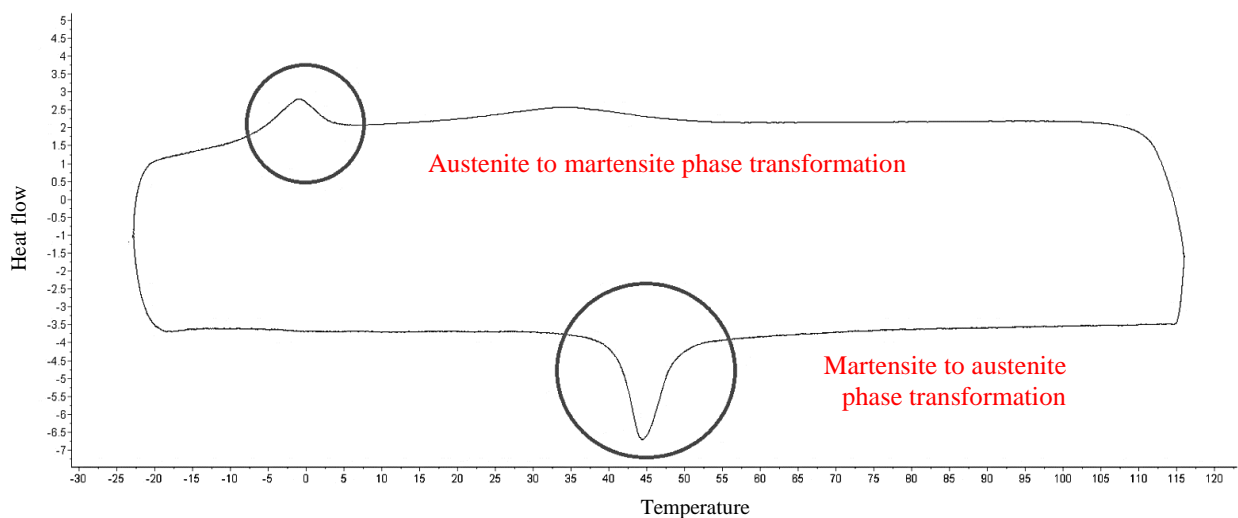
Figure 33. Heat flow against temperature results of DSC test.

41

CHAPTER VI

6. JOINT DESIGN

This section will provide a more detailed and target-oriented presentation of the design approach. In the concepts section, different proposed designs were discussed and analyzed. Selected conceptual design was then studied and dissected into design elements which needed further detail. Structurally the chosen system comprises four different elements. NiTi wires which provide actuation forces will be examined in relation to one another. Couplings at two ends are identical in design and manufacturing and their shape identifies relative position of other elements. Lastly, the coil spring design according to its objectives will be showcased.

6.1. Actuating SMA Wire

Shape memory alloy heat treatment conditions were defined in the previous section. Other than the temperature and duration of heat treatment the imprinted shape memory is of importance. To induce bending motion, first actuating wire needs to memorize a bent shape. 90 degrees of bending is the extreme goal while normal performance condition is 60 degrees. To fulfill this and simultaneously not transgress the 8% strain limit, bending wire can theoretically be treated up to 140 degrees as discussed in Chapter IV. Similarly, for the resetting wire a range from -50 to 0 degrees is acceptable, considering the bending target of 90 degrees. Compatibility of different bending and resetting combinations were then experimentally investigated. Table 3 demonstrate the steps in which the samples were combined and their performance has been checked and their maximum bent (B) and reset (R) values are listed.

Table 3. Minimum and maximum performance values of different bending and resetting wire combinations.

		Resetting treatment as ratio of resetting target	
		1	1.2
Bending treatment as ratio of bending target	1	B= 0.7, R=0.8	B= 0.63, R=1.1
	1.1	B= 0.75, R=0.77	B= 0.72, R=1.09
	1.2	B= 0.82, R=0.75	B= 0.80, R=1.07
	1.3	B= 0.94, R=0.74	B= 0.91, R=1.04
	1.4	B= 1, R=0.72	B= 0.99, R=1.04
	1.5	B=1.16, R=0.70	B= 1.11, R=1.03

Figure 34 presents the performance of a bending and resetting sequence for each combination mentioned above. Each sample was fixed into actuation setup and heated with a current of 2.5 A.

It is deduced from the figures that a bending wire with the memory of 1.5 times the target angle is the only one providing sufficient moment to bend the joint up to 90º and possibly beyond. Consequently, it is proven that a straight memory for the bending wire will not reset the joint to initial position. On the other hand, a resetting wire trained for 1.2 times the target resetting, while limiting the bending range, is capable of achieving full reset. Thus, combination of 1.5 bending wire and 1.2 resetting wire is poised as the satisfactory choice.
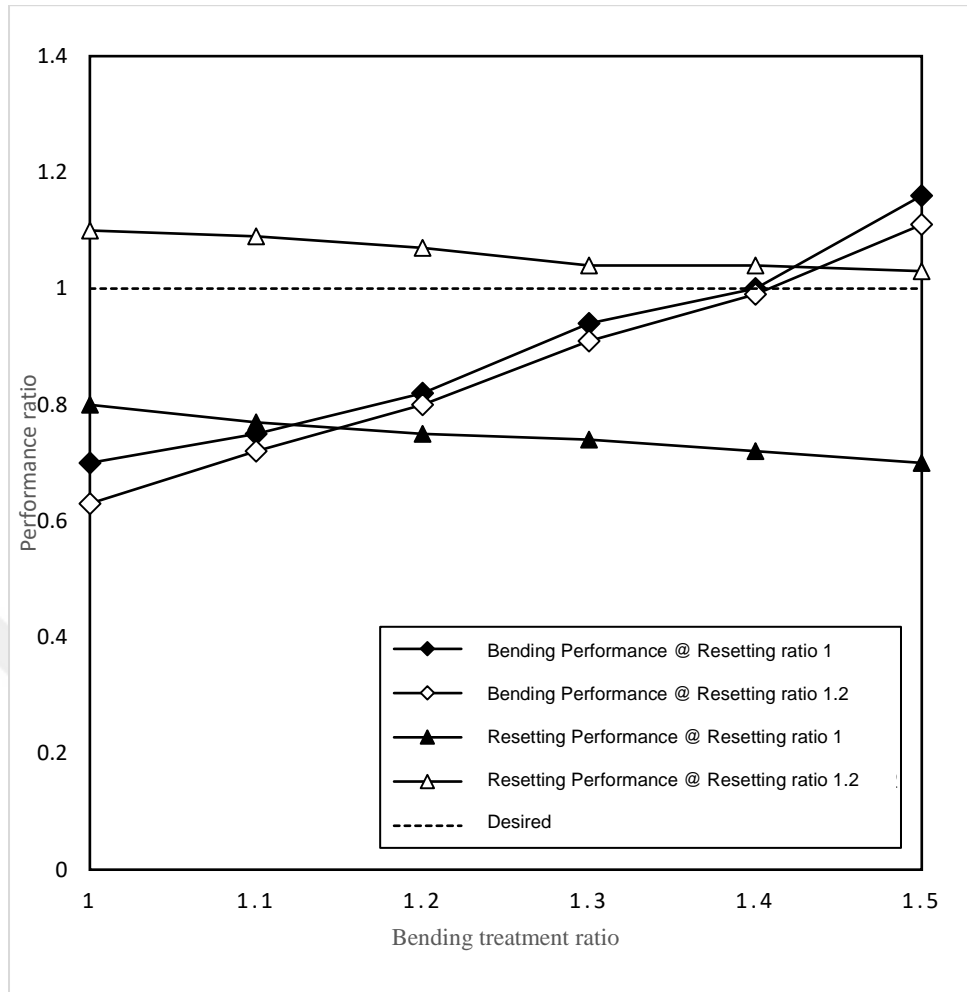
Figure 34. Bending and resetting capacity of different bending and resetting wires combined.

6.2.   Coil Spring

Coil springs propose a geometrical constraint at bent shape. While bending, every coil can form an arc of a limited angle, due to difference between inner and outer radius of curvature. It is crucial to calculate the maximum solid length allowed. This allowable solid length will be the inner arc length of a 90º bent joint if the bending NiTi wire is positioned at the outer arc. If R is the outer and r the inner radius and L and l (Figure 35) present the respective arc lengths, the following calculation provides the maximum solid length of the spring.
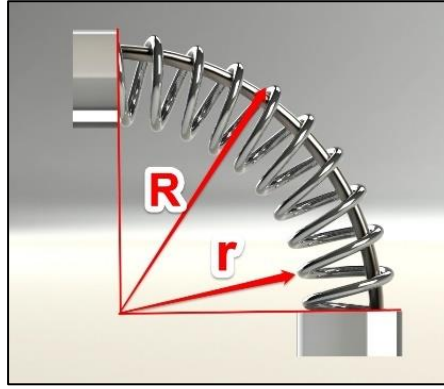
Figure 35. Three-dimensional depiction of different radii of curvature

The compressed length of spring (l) can be calculated as 4.5 mm from geometric relations. The same value can also be determined by multiplying the spring wire diameter by the total active coil number.

Resistive force induced by coil spring can be calculated using Hooke's law of springs. In order to apply it to the bending coil, the coil has been considered as a circular arrangement of differential springs. Compression or extension of each differential can be calculated using the geometric arc length relations. Consequently, the total force of this arrangement can be calculated as integral multiplication of differential spring constants with differential deformations. Springs are parallel then K=dK*m in which m is the total number of differential springs and dK is the differential spring constant. Assuming m is an integer number we can write the integral as a series calculation, $F = \frac{K}{m}[\sum_{i=1}^{m} \delta L_i]$.

This calculation can be simplified if the total deflection of the spring is assumed as average of absolute maximum and minimum length change in the spring, with negligible error. Hence, the force of a spring in bending will be estimated as follows. L is equal to the bending length and D is the inner coupling diameter ($F \approx kLD$). Consequently, the moment that spring exerts on the NiTi wire can be estimated as follows ($M \approx kLD^2$).

Structurally, the rate value of a spring is calculated as below, providing design parameters are calculable if the rate value needed can be estimated, where G is the modulus of rigidity, d the wire diameter, D the mean coil diameter; and n is the active coil number.

$$K = \frac{F}{\Delta L} = \frac{G.d^4}{8.D^3.n}$$

Experimentally it is observed that NiTi bending wire can perform under the effect of 1N of load. The maximum deflection of the coil spring in the joint can be estimated as 5.5mm. Having these two values the maximum allowable spring rate can be estimated as 0.18 N/m.

As two sample materials, common for spring makers, stainless steel of 0.2 and 0.3 mm have been provided for the project. Lower limit and upper limit for number of coils are respectively related to maximum rate value and maximum solid length (Table 4).

Table 4. Upper and lower limit of allowable coil numbers according to spring wire diameter.

		For k = 0.18	For solid length = 4.5 mm
Wire Diameter	0.2 mm	Coil number = 2	Coil number = 22.5
	0.3 mm	Coil number = 10.5	Coil number = 15

Since the 0.3mm wire is easier to handle in manufacturing while having a smaller range of allowable coil numbers a spring made by the 0.3mm wire and 12 active coil numbers is chosen. Twelve coils will simultaneously provide extra space for occasional actuations above 90º to reduce possible damage (Figure 36).

Figure 36. Picture of a coil spring made of 0.3mm stainless steel wire.

6.3.   Coupling

In this stage with spring and NiTi wires designed, couplings will be holding the system together and govern their relative placement. As explained in the conceptual design, coupling must position both wires closest possible to the inner wall of the coil spring and farthest from the horizontal centerline of the joint.

Fitting two wires at the least distance from this point faces two restrictions. Electrical connections and respective attachments to each wire needs to be considered. Thinnest available wire which can endure currents needed has 5mm coated and 0,3mm uncoated diameter. At the same time, ventilation and thermal independence of each wire are important. Sole driving force for NiTi actuation is material temperature. If wires cannot have different temperatures and heat transfer occurs, independent actuation of one wire without triggering phase transformation in the opposition is extremely difficult. A minimum distance is needed to eliminate conductive heat transfer and provide performance independence. Having both wires at one side will also leave the rest of the internal space for wiring and extra passage way.
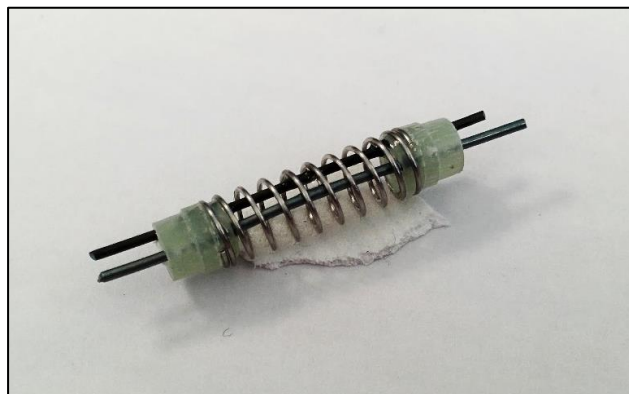
Figure 37. Picture of a joint comprising of two couplings, two NiTi wires and one coil spring.

To fix the spring securely at both ends a ridge is placed at the coupling inner face. Outside part of each coupling can be elongated according to the need employing the actuator joint.

CHAPTER VII

7. RESULTS AND DISCUSSION

Having the final joint design, several sample joints were assembled and their performance were exhibited. Experimental setup structure has been explained in Chapter IV. Samples are fixed in the setup and attached to the programmable power supply. Each wire in the joint is then attached to a T-type thermocouple. Experimental cyclic test program (Section 4.3.) actuates the bending wire at the beginning and after reaching the set bending angle waits for the system to cool down to 25°C and then activates the resetting wire until straight position is achieved.

7.1. Single actuation behavior

Figure 38 presents behavior of joints in one actuation cycle for different set bending angles.
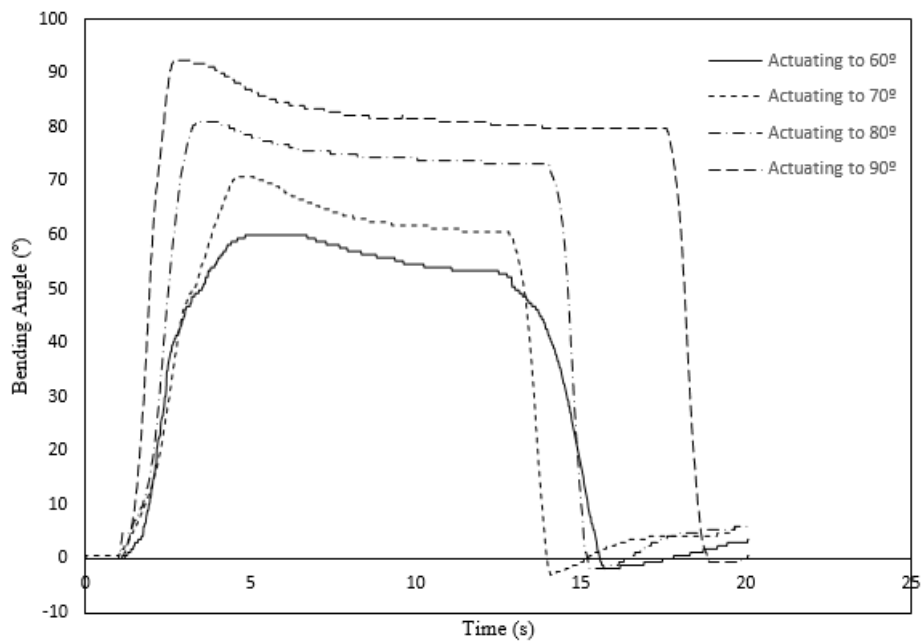
Figure 38. Performance of a joint when set for different bending angles.

Cycle starts with heating the bending wire, then the cool-off stage begins. Resetting wire is only activated after system is back at 25ºC and finishes when 0º is realized. Cool-off duration extends with the increase of set bending angle as expected. If the samples are similar in design and treatment, a higher temperature would be needed for bending 90º in comparison to 60º. Hence, a longer period will be needed to reach 25ºC in return. Bending and resetting stages of the cycle poses comparable slopes which is in line with consistency of different samples.
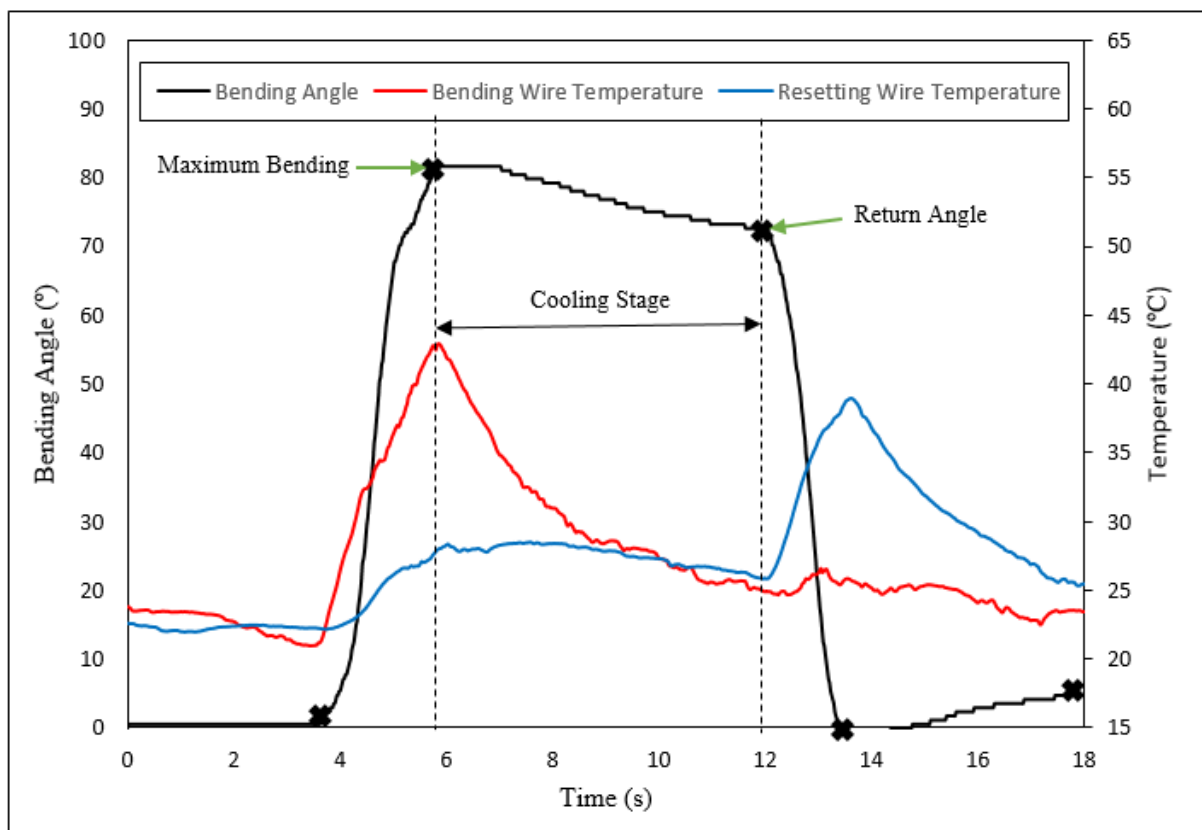
Figure 39. Investigation of one cycle of actuation according to NiTi wire temperature.

Figure 39 depicts a transposition of the changes in bending angle and wire temperatures with time. Slightly lower temperature values for resetting wire is justified by the presence of the coil spring in the system. Although dynamic effects of the spring do not hamper functioning of the actuator, it does cause an inclination toward straight position. This minute

effect is for the resetting and against the bending motion, which causes the slight difference between maximum temperature of bending wire and resetting wire, the former being larger.

7.2. *Cyclic behavior of the joint*

It is already established in the previous section, that the joint is suitable for performing one single bending and resetting cycle of different target values. However, antagonistic actuators are well-documented to undergo degradation when actuated cyclically [51]. Sofla et al. have observed the cyclic behavior of a similarly antagonistic structure powered by NiTi wires in detail and have reported a diminishing trend in shape recovery of the actuator which is referred to as a logarithmic decrease in actuators stroke [51]. Stroke of a shape memory actuator is defined as the shape recovery due to phase transformation, which is the propellant force of any SMA included actuator.
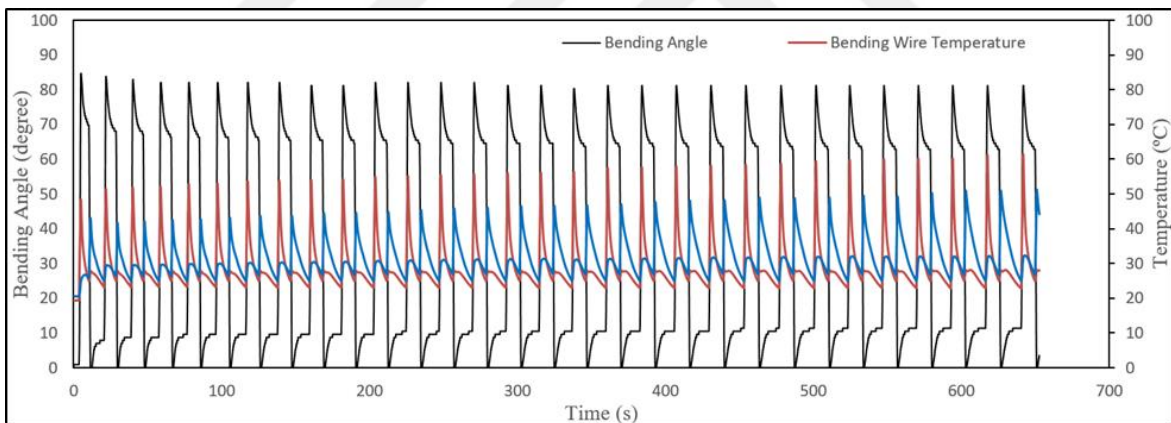
Figure 40. Recorded bending angle and bending wire temperature during a cyclic test

To better study the behavior of the proposed active joint series of cyclic tests are designed and performed via the aforementioned experimental setups. Each wire temperature is observed and recorded as the cyclic test proceeds. Hence, the electrical current is controlled according to these temperature values. Deformation of the joint is also recorded via an encoder which is also a mean of controlling cyclic actuations.

Figure 40 is representative of one full test of 30 cycles of bending to 80° and resetting back to 0°. Moreover, detailed changes in the temperature of the both wires are also depicted in the same figure. It is worth noting that the maximum temperature of the wire in each cycle increases as the number of cycles increase. It can be deduced that higher temperature of bending wire was required in order to reach the same bending angle of 80° within the next cycles.

This behavior was also reported for NiTi shape memory alloy elsewhere [51]. In the aforementioned research work by Sofla et al., maximum temperature of 100°C (above austenite finish temperature (A_f)) was utilized for activating the SMA wires during the cyclic tests. It was observed that strain values noticeably decrease with the increase of cycle numbers. To be more exact, higher temperature would be needed to obtain greater deformation. It was also reported that after a number of actuation cycles this degradation of the actuator stroke stabilizes [51]. It was shown that phase transformation stroke decreases logarithmically. Such a behavior was rationalized in terms of the increased localized deformation [52,53]. It is well-known that stress induced martensite can be formed during the cyclic test leading to the formation of localized deformation in the vicinity of residual martensite plates [52]. The interactions between stress fields of these localized deformations act against phase transformation. Therefore, formation of non-recoverable martensite plates at each cycle describe the cyclic hardening. This behavior is in line with the observed increase in maximum bending wire temperature against cycle number (Figure 41).
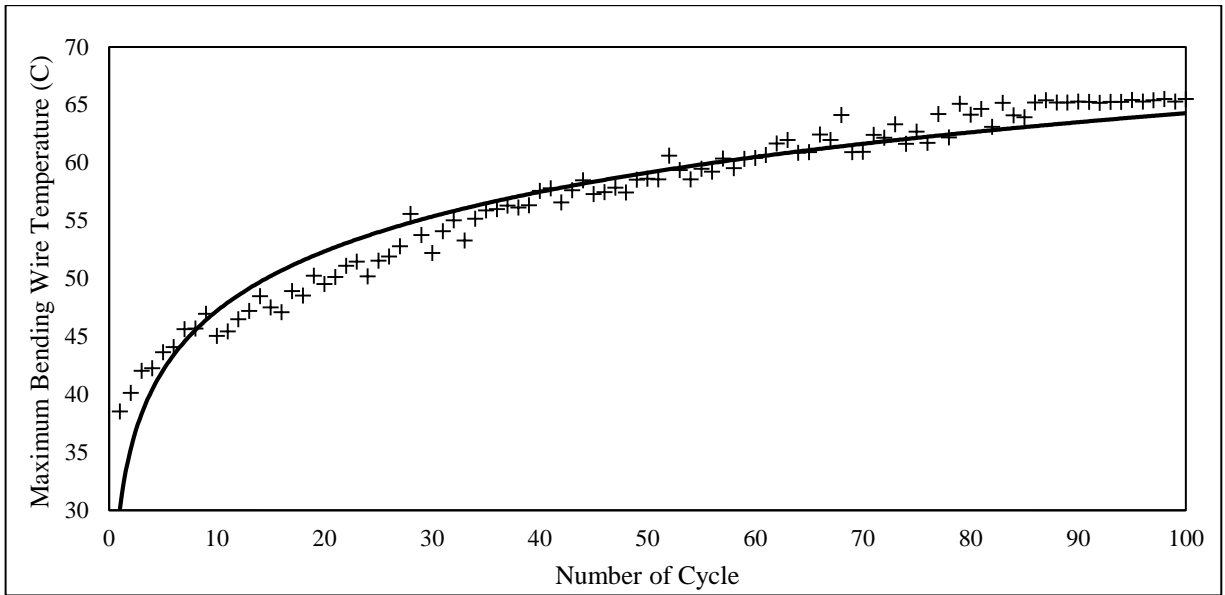
Figure 41. Maximum temperature of the bending wire recorded in each cycle for a 100 cycle test of bending to 60° and resetting to 0°
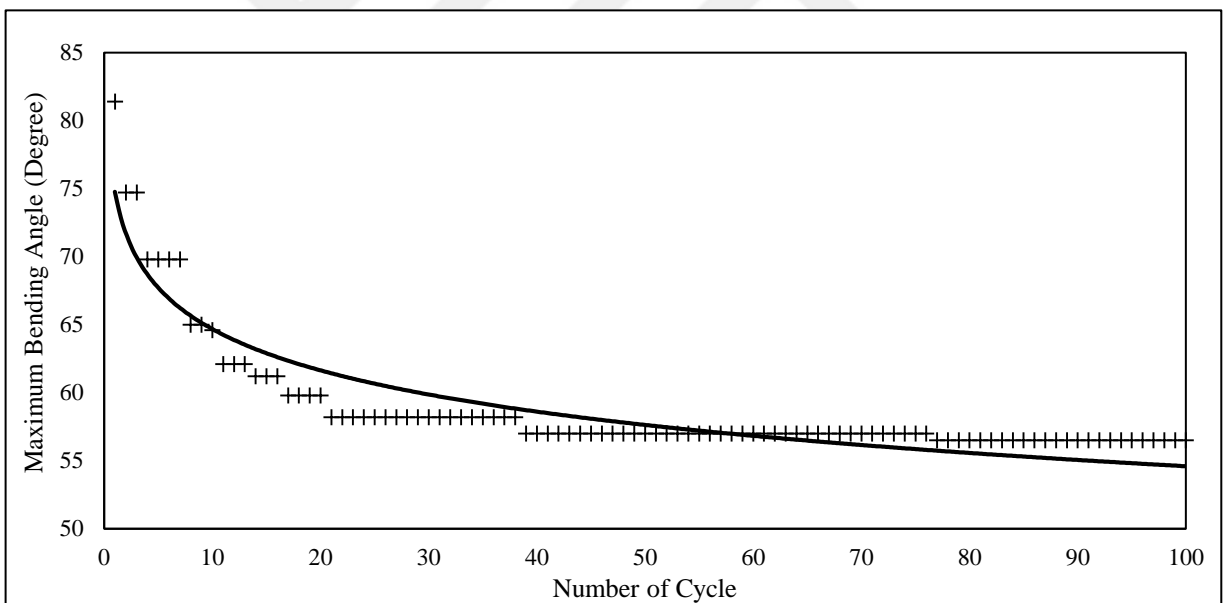
Figure 42. Maximum bending reached at each cycle when heated up to 45°C while actuation

To further confirm the correlation between the observed increase of temperature peaks and the diminishing actuator stroke, another cyclic test has been performed in which the peak temperatures were kept at constant values while recording the bending of the joint.

Figure 42 is a sample representation of one of these evaluation cyclic tests in which the peak temperature is kept at temperature below austenite finish. Recorded performance results lie in accordance to the literature observations and change of maximum bending angle can be logarithmically related to the number of cycles.

Consequently, it is also observed in the cyclic test graphs (Figure 40) that in cooling step of each cycle, the joint experiences a reverse deformation after both bending and resetting stage. It is also recorded that the amplitude of this reverse deformation grows measurably with the number of cycles.

Figure 43. Representation of the final value of cooling stage return angle after bending at each cycle in cyclic test with target angle of 60.

Figure 43 and 44 represent the reverse deformation angles of the joints during cooling stage (electrical current off time) after bending and resetting actuations, respectively. Obviously, gap between the target and return angles (i.e., reverse deformation) considerably increased with the rise in cycle number. One of the main reasons for such an observation can be imputed to the variation in the actuation temperature of each cycle. As discussed earlier, temperature of subsequent cycles increased in order to reach to the same bending or resetting

54

target angle. Oregeas et al. considered the effects of temperature on the cyclic response of NiTi [54]. It was reported that stress levels are higher at elevated temperatures. Simultaneously, it has been reported that yield stress of these alloys tend to decrease as a result of cyclic deformations [55,56].
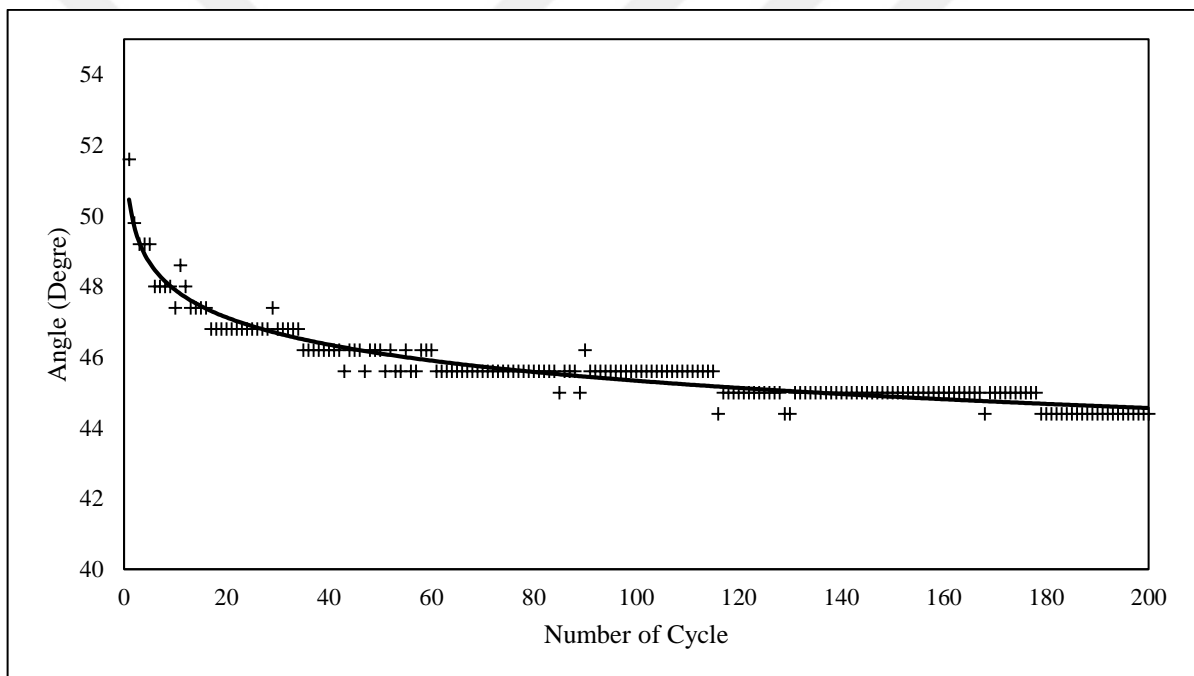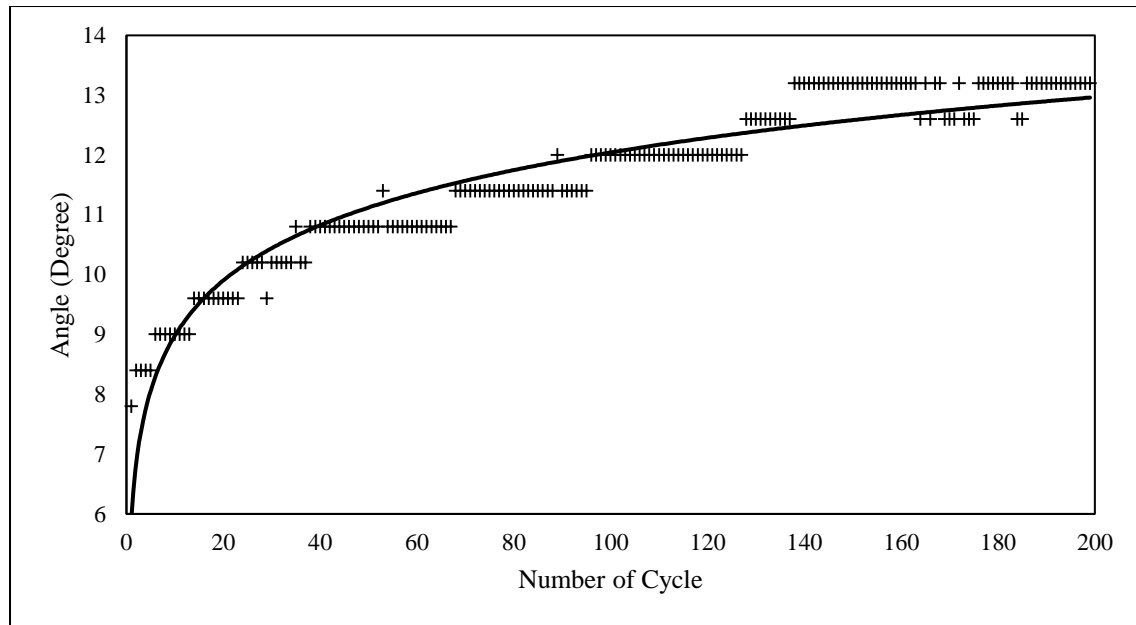

Figure 44. Representation of the final value of cooling stage return angle after resetting at each cycle in a cyclic test with target angle of 60.

Another participating element to this phenomenon is the resisting moment exerted by the antagonist wire which is supposedly inactive. But due to residual convective heat transfer inside the joint, it is measured that the temperature of the opposing wire also slightly increases as the temperature of the bending wire rises during the actuation. Figure 40 also depicts this slight rise of temperature during the cooling stages of each cycle. Simultaneously, it is observable that peak of this slight temperature rise during the opposite actuation, increases with the number of cycles. This makes the opposing stress on the just actuated wire (bending or resetting) magnified after each cycle. This increase in the opposing stress coupled with lower yield stress value of the wires in later cycles contributes to further diminishing the bending or resetting angle during the cooling stage.

Figure 45 is a comparison between slopes of changes in the bending angle during the cooling stages of first and 100th cycle of a cyclic test with the target angle of 60°. Higher magnitude of the slope in the last cycle is in fine agreement with the mentioned discussions for increase of reverse deformation angle with the number of cycles.

Figure 45. Comparison of the reversing slope between 1st and 100th cycle of a test with target angle of 60°.

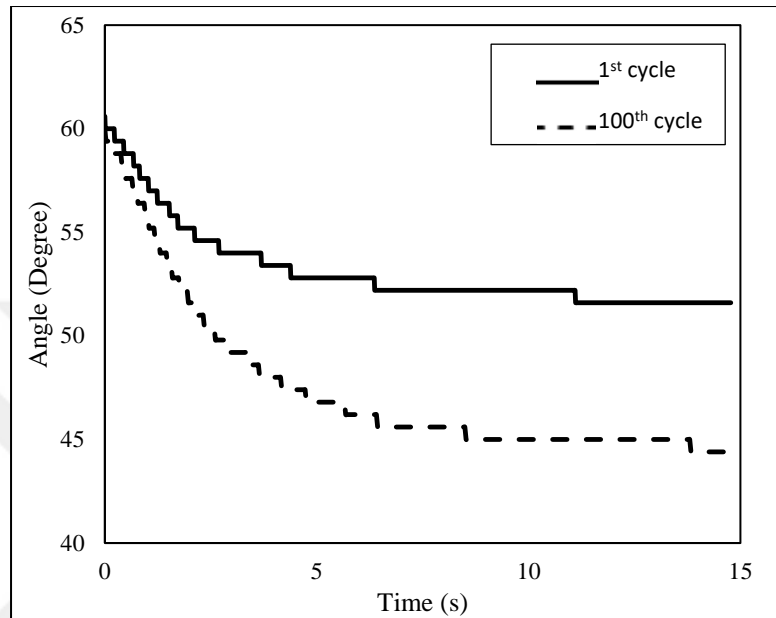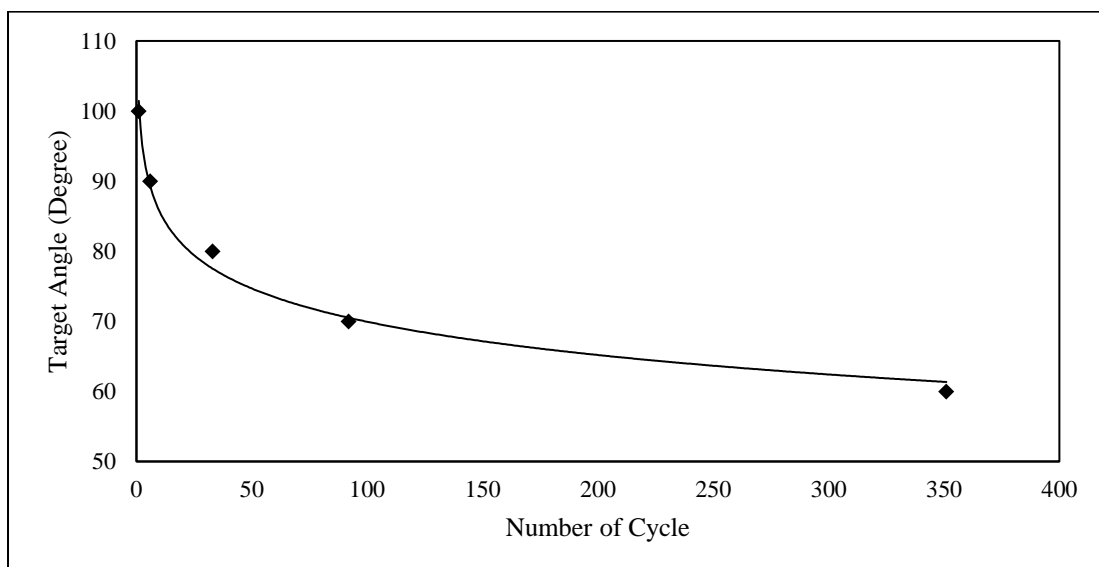Figure 46. Fatigue performance of the antagonistically actuated joint

56

All these evidences point to a gradual degradation of antagonistic behavior which call for the demonstration of cyclic performance and subsequent failure. Hence, a failure standard can be described for the current active joint as the incapability of achieving the target set angle during cyclic actuation. Accordingly, cyclic tests were performed for different targets in order to document the fatigue performance. The discussion presented so far proves the existence of degrading actuation behavior during cyclic by outlining the possible underlying reasons. Figure 46 also depicts the effect of target bending angle on catalyzing the functional fatigue in the actuator.

To better explain the fatigue performance, three sets of cycle tests were devised. Each cycle set encompassed a different target angle and for each target angle, four different cycle numbers, were tested below the failure limits shown in Figure 46. After cyclic experiments, the actuated joints were disassembled to individual components. Then, the two wires at the heart of each joint were individually investigated and characterized to attain ample information about the implications of cyclic actuation.
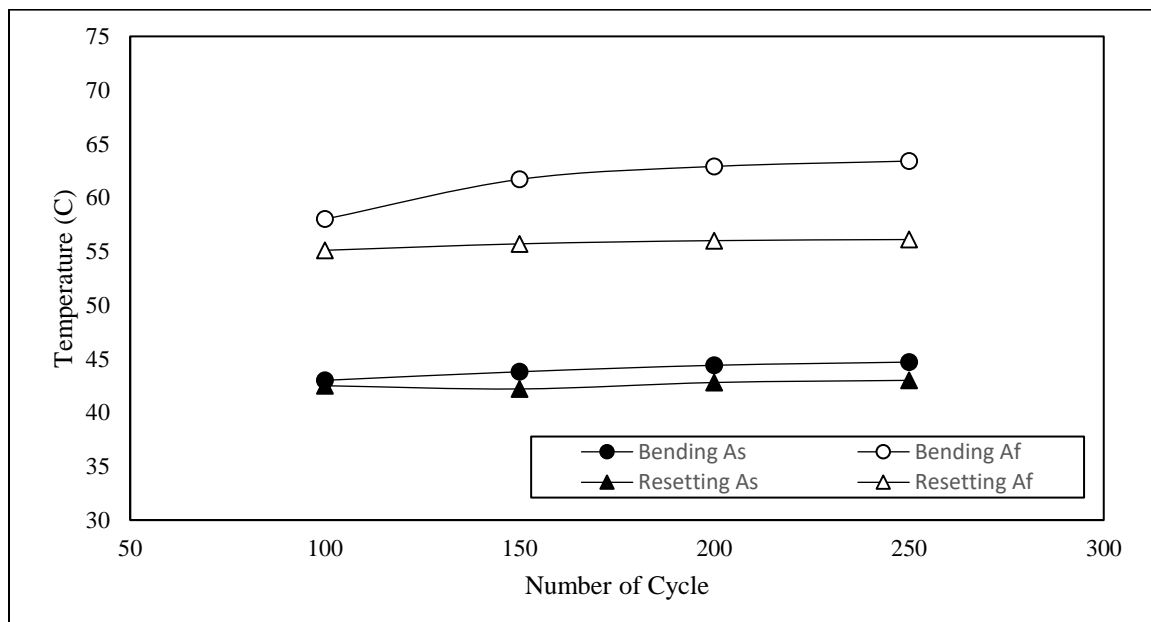
Figure 47. Austenite phase transformation temperature changes in cyclic performance with target angle of 60° (austenite start and finish temperatures).
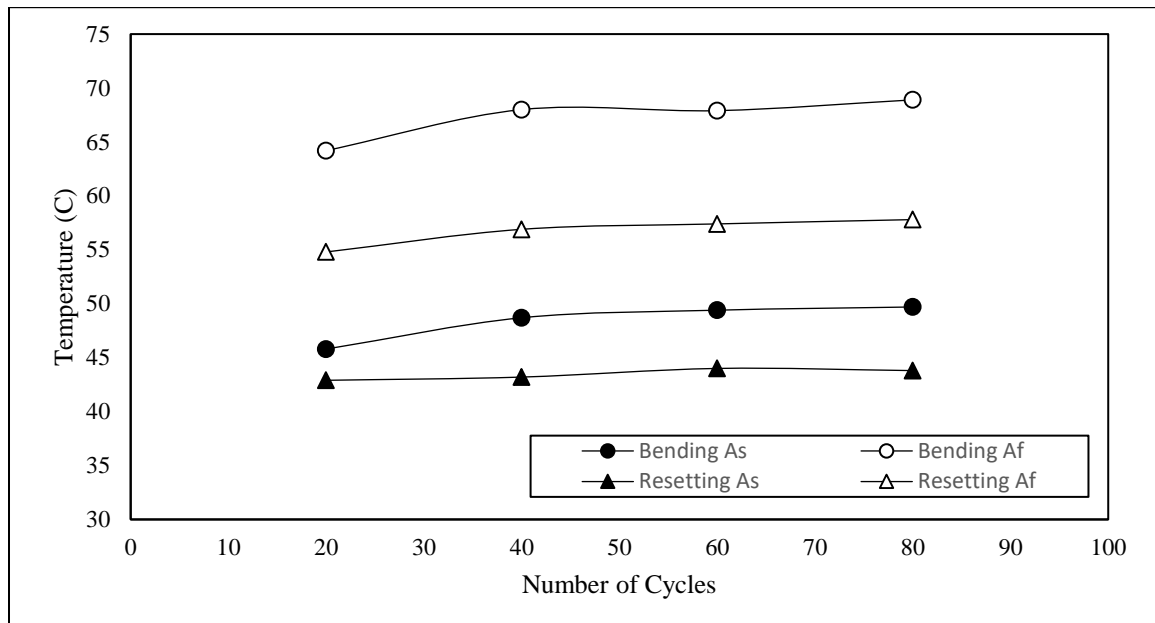
Figure 48. Austenite phase transformation temperature changes in cyclic performance with target angle of 70° (austenite start and finish temperatures).
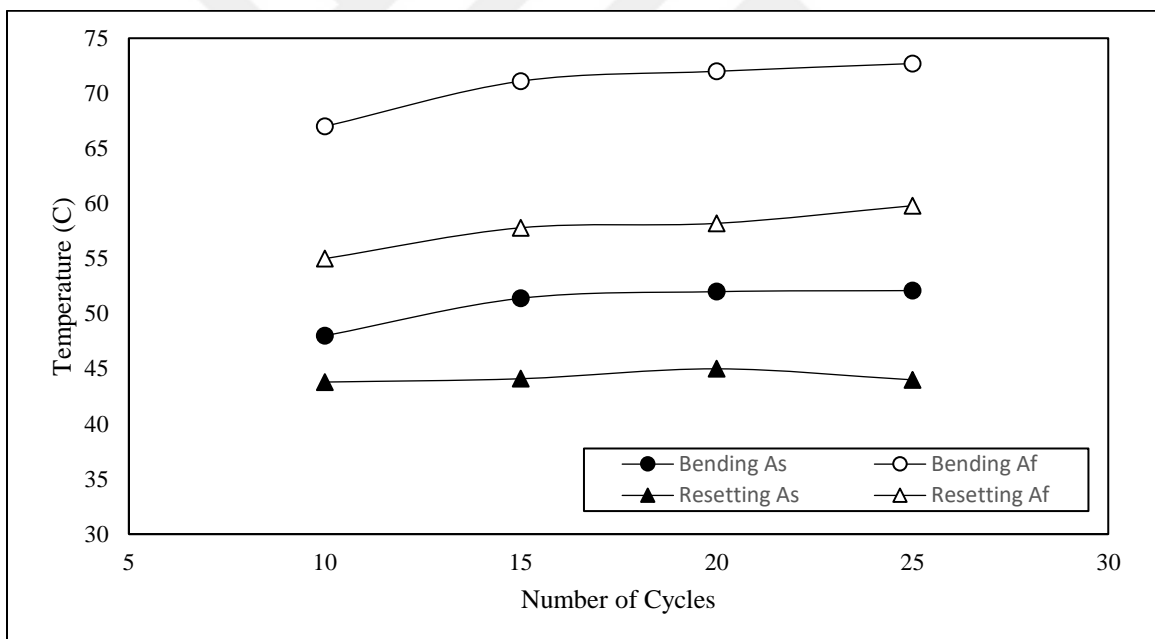
Figure 49. Austenite phase transformation temperature changes in cyclic performance with target angle of 80° (austenite start and finish temperatures).

Accordingly, Figures 47-49 demonstrate the changing trait in the transformation temperatures of the austenite phase against cycle number for each target angle. These transformation temperatures have been acquired according to bend and free recovery method [57]. It is observed that transformational temperatures rise with the number of cycles

performed and the actuation to higher target bending angle results in steeper shift of these temperatures to higher values. This trend is also in line with the rising maximum temperature at each cycle as the number of cycles increase.

Disassembled individual SMA wires were also tested with the load cell setup in an attempt to better understand the fatigue behavior of the material. As Figures 50-52 clearly represent, the hysteresis in temperature-force graphs of these wires increase with the cycle number. Hysteresis growth is in turn caused by increased energy dissipation in the material [58] which is in turn an indicator for worse fatigue behavior. Occurrence of load hysteresis in individual wires is in conformance with the degradation of the joint cyclic performance. The observed contrast between changes in hysteresis value for resetting wire can be attributed to their limited shape recovery due to their near straight treatment, which in turn limits the reading of their force values. The bending SMA wires also show a decrease in recoverable deformation by phase transformation with both increase of cycle number and actuation angle (Figure 53). This is another indication of the reduced joint target angle with number of actuation cycles.

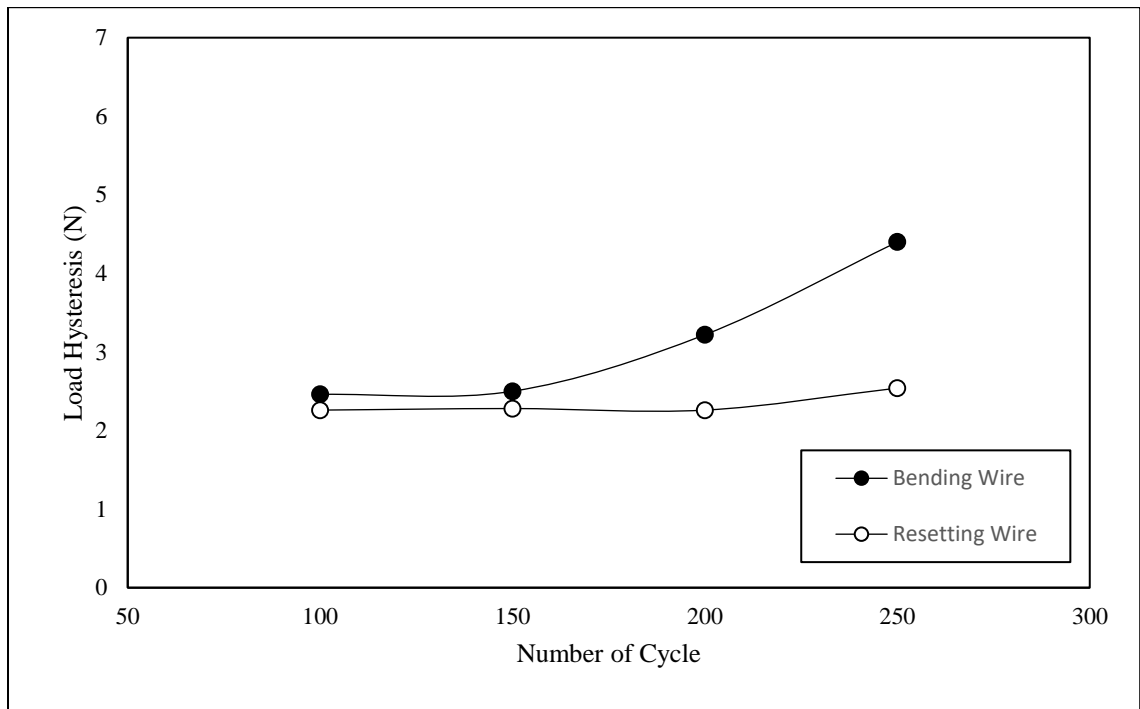Figure 50. Load hysteresis changes against number of cycles for target angle of 60°
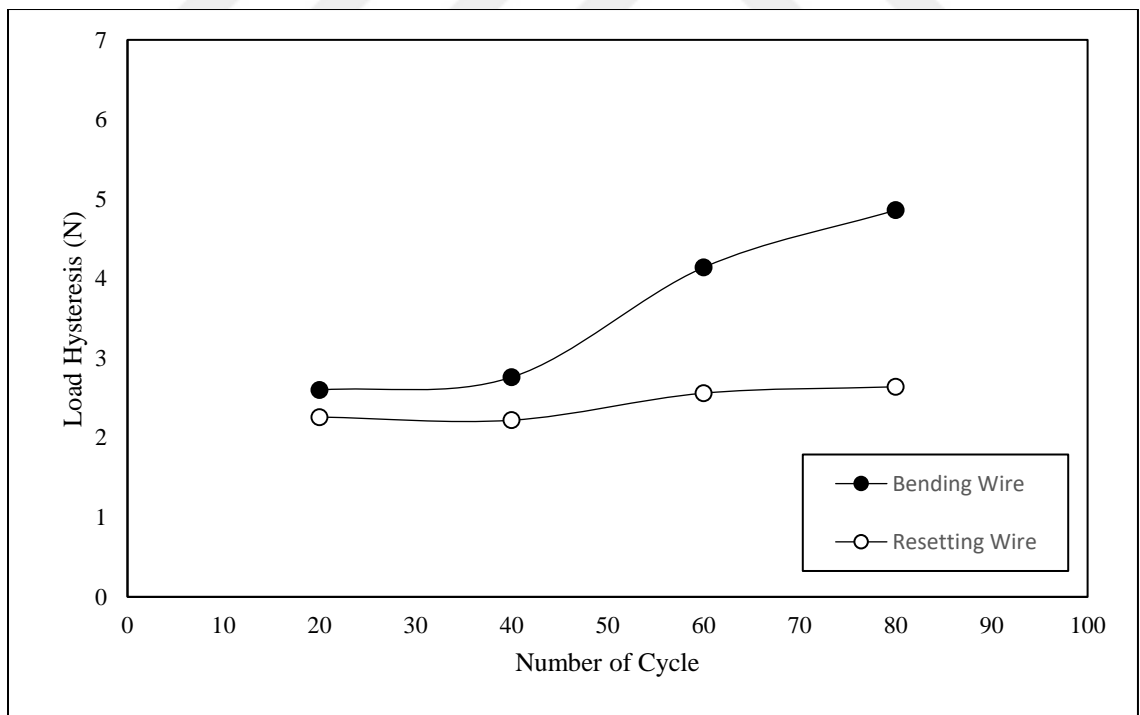

Figure 51. Load hysteresis changes against number of cycles for target angle of 70°
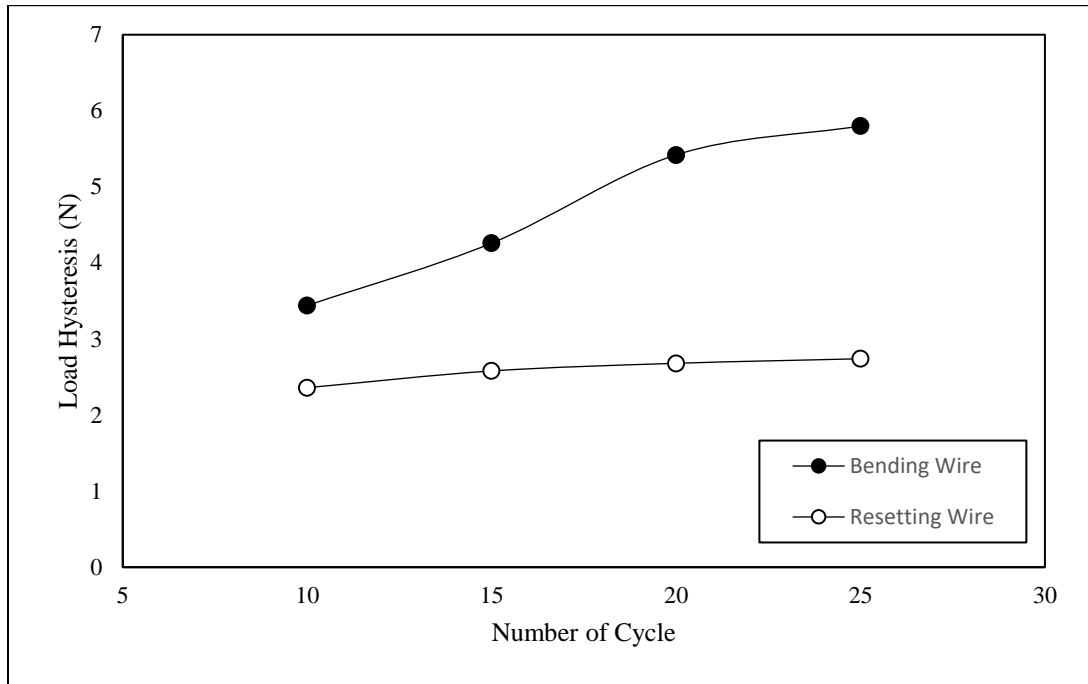
Figure 52. Load hysteresis changes against number of cycles for target angle of 80°
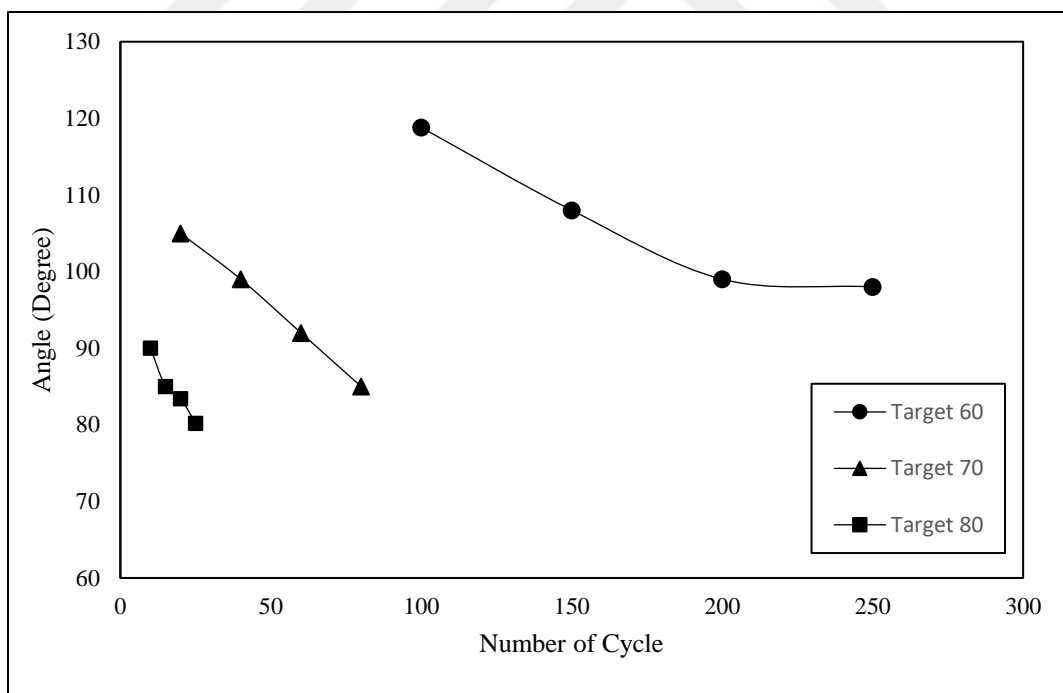
Figure 53. Maximum achievable recoverable deformation for bending wire after cyclic performance.

CHAPTER VIII

8. CONCLUSIONS

An antagonistically actuated active joint by an SMA wire couple is designed and manufactured. The joint is comprises of two wires which are heat treated at 500ºC to attain a relatively lower set of transformation temperatures while having the minimum difference between austenite start and finish temperatures. Then it is experimentally established that bending wire must be treated while bent into 1.5 times the bending target angle and respectively the resetting wire into 1.2 times the resetting target angle. Wires are fixed together at two ends with a set of couplings which are designed to provide parallel actuation planes. The joint is enveloped with a coil spring. Presence of a damping component can provide a physical bridge between the actuator wires while enhancing controllability and tracking characteristics of the joint.

The joint is capable of attaining bent shapes up to 100°. As a mandatory step in trials of any actuator, joints are tested in various cyclic conditions. It is then revealed that cyclic actuation results in degradation of the joint bending angle and limits its range of motion. During cyclic actuation, higher temperatures are needed to achieve the target bending angle at each cycle in comparison to the previous one. This is attributed to the localized deformation in the vicinity of residual martensite plates. Stress fields surrounding these deformation regions tend to interact and impede phase transformation. With increased target angle, the number of cyclic actuations decreases.

Moreover, it is observed that in cooling stages of each cycle a portion of the target deformation is reversed. This tendency increased with the number of cycles. This is also linked with diminishing yield stress of the alloy with cycle number and also increase of the peak temperature. Due to heat transfer between the wires the antagonist wire also rises to a

porsion of the actuation wire temperature which increases the stress applied against actuation which in turn contributes to reverse deformation. Properties of individual wires are tested after cyclic performance. It is demonstrated that transformation temperatures as well as stress hysteresis of the material also increase with the number of actuation cycles. As a result, characterization of the cyclic behavior of active joint is carried out. Degradation in cyclic performance was linked with the fatigue of individual wires as possibly related to increased energy dissipation.

These actuators have the capacity of being included in different robotic structures and controllability of them need further research. Moreover, a detailed microstructural study of the actuators before and after cyclic performance can additionally prove the mentioned performance trends. Consequently, further research on effects of coupling design and heat treatment on cyclic performance of joints can be conducted. Also, investigation of possible advantages in two-way shape memory effect for such joint is beneficial.

REFERENCES

[1]   Lagoudas D C 2007 *Shape Memory Alloys* (Springer)

[2]   Hodgson D E, Wu M H and Biermann R J 1990 Shape Memory Alloy *(ASM Int.* **2** 897–902

[3]   Thompson S A 2000 An overview of nickel-titanium alloys used in dentistry. *Int. Endod. J.* **33** 297–310

[4]   Ōtsuka K and Wayman C M 1999 *Shape memory materials* (Cambridge University Press)

[5]   Calhoun C 2012 *Actuation Fatigue of Shape Memory Alloys* (Texas A&M University)

[6]   Shaw J A and Kyriakides S 1995 Thermomechanical Aspects of NiTi *J. Mech. Phys. Solids* **43** 1243–81

[7]   Mihálcz I 2001 Fundamental characteristics and design method for nickel-titanium shape memory alloy *Period. Polytech. Mech. Eng.* **45** 75–86

[8]   Nemat-Nasser S and Guo W G 2006 Superelastic and cyclic response of NiTi SMA at various strain rates and temperatures *Mech. Mater.* **38** 463–74

[9]   Stoeckel D 1995 The Shape Memory Effect - Phenomenon, Alloys, and Applications *Shape Mem. Alloy. Power Syst. EPRI* **683** 1–13

[10]   Miller D A and Lagoudas D C 2001 Influence of cold work and heat treatment on the shape memory effect and plastic strain development of NiTi *Mater. Sci. Eng. A* **308** 161–75

[11]   Yeung K W K, Cheung K M C, Lu W W and Chung C Y 2004 Optimization of

thermal treatment parameters to alter austenitic phase transition temperature of NiTi alloy for medical implant *Mater. Sci. Eng. A* **383** 213–8

[12]　Liu Y and McCormick P G 1989 Influence of heat treatment on the mechanical behaviour of a NiTi alloy. *ISIJ Int.* **29** 417–22

[13]　Huang X and Liu Y 2001 Effect of annealing on the transformation behavior and superelasticity of NiTi shape memory alloy *Scr. Mater.* **45** 153–60

[14]　Mitwally M E and Farag M 2009 Effect of cold work and annealing on the structure and characteristics of NiTi alloy *Mater. Sci. Eng. A* **519** 155–66

[15]　Ho M and Desai J P 2009 Characterization of SMA actuator for applications in robotic neurosurgery *Proceedings of the 31st Annual International Conference of the IEEE Engineering in Medicine and Biology Society: Engineering the Future of Biomedicine, EMBC 2009* pp 6856–9

[16]　Fumagalli L, Butera F and Coda A 2009 SmartFlex NiTi wires for shape memory actuators *J. Mater. Eng. Perform.* **18** 691–5

[17]　Ikuta K 1990 Micro/miniature shape memory alloy actuator *Proceedings., IEEE Int. Conf. Robot. Autom.* 2156–61

[18]　Calhoun C, Wheeler R, Baxevanis T and Lagoudas D C 2015 Actuation fatigue life prediction of shape memory alloys under the constant-stress loading condition *Scr. Mater.* **95** 58–61

[19]　Williams E and Elahinia M H 2008 An Automotive SMA Mirror Actuator: Modeling, Design, and Experimental Evaluation *J. Intell. Mater. Syst. Struct.* **19** 1425–34

[20]　Holschuh B and Newman D 2014 Low spring index, large displacement Shape Memory Alloy (SMA) coil actuators for use in macro- and micro-systems *SPIE*

MOEMS-MEMS ed H R Shea and R Ramesham (International Society for Optics and Photonics) p 897505

[21]   Ōtsuka K and Wayman C M 1999 *Shape memory materials* (Cambridge University Press)

[22]   Huang W 2002 On the selection of shape memory alloys for actuators *Mater. Des.* **23** 11–9

[23]   Ikuta K, Tsukamoto M and Hirose S 1988 Shape memory alloy servo actuator system with electric resistance feedback and application for active endoscope *Proceedings. 1988 IEEE Int. Conf. Robot. Autom.* 427–30

[24]   Bergamasco M, Dario P and Salsedo F 1990 Shape Memory Alloy microactuators *Sensors Actuators A* 253–7

[25]   Lee Y-J, Son H-M, Gu J-B and Nam T-H 2006 Design and control of multi-step SMA actuator *Int. J. Appl. Electromagn. Mech.* **23** 119–24

[26]   Grant D and Hayward V 1995 Design of shape memory alloy actuator with high strain and variable structure control *IEEE Int. Conf. Robot. Autom.* 2305–12

[27]   Benard W L, Kahn H, Heuer A H and Huff M a. 1997 A titanium-nickel shape-memory alloy actuated micropump *Proc. Int. Solid State Sensors Actuators Conf. (Transducers '97)* **1** 3–6

[28]   Kahn H, Huff M A and Heuer A H 1998 The TiNi shape-memory alloy and its applications for MEMS *J. Micromech. Microeng* **8** 213–21

[29]   Icardi U 2001 Large bending actuator made with SMA contractile wires: Theory, numerical simulation and experiments *Compos. Part BEngineering* **32** 259–67

[30]   Wang G and Shahinpoor M 1997 Design, prototyping and computer simulations of a novel large bending actuator made with a shape memory alloy contractile wire *Smart Mater. Struct.* **6** 214–21

[31]   Sofla a. Y N, Elzey D M and Wadley H N G 2008 Two-way Antagonistic Shape Actuation Based on the One-way Shape Memory Effect *J. Intell. Mater. Syst. Struct.* **19** 1017–27

[32]   Wang Z, Hang G, Li J, Wang Y and Xiao K 2008 A micro-robot fish with embedded SMA wire actuated flexible biomimetic fin *Sensors Actuators, A Phys.* **144** 354–60

[33]   Kuribayashi K, Tsuchiya K, You Z, Tomus D, Umemoto M, Ito T and Sasaki M 2006 Self-deployable origami stent grafts as a biomedical application of Ni-rich TiNi shape memory alloy foil *Mater. Sci. Eng. A* **419** 131–7

[34]   Lim G, Park K, Sugihara M, Minami K and Esashi M 1996 Future of active catheters *Sensors Actuators A Phys.* **56** 113–21

[35]   Haga Y, Mineta T, Totsu K, Makishi W and Esashi M 2001 Development of Active Catheter, Active Guide Wire and Micro Sensor Systems *Interv. Neuroradiol.* **7** 125–30

[36]   Haga Y, Esashi M and Maeda S 2000 Bending, torsional and extending active catheter assembled using electroplating *Proc. IEEE Thirteen. Annu. Int. Conf. Micro Electro Mech. Syst. (Cat. No.00CH36308)* 181–6

[37]   Mineta T, Mitsui T, Watanabe Y, Kobayashi S, Haga Y and Esashi M 2002 An active guide wire with shape memory alloy bending actuator fabricated by room temperature process *Sensors Actuators, A Phys.* **97**–**98** 632–7

[38]   Takizawa H, Tosaka H, Ohta R, Kaneko S and Ueda Y 1999 Development of a

microfine active bending catheter equipped with MIF tactile sensors *Micro Electro Mechanical Systems, 1999. MEMS '99. Twelfth IEEE International Conference on* pp 412–7

[39]   Haga Y, Mineta T, Makishi W, Matsunaga T and Esashi M 1998 Active Bending Catheter and Endoscope Using Shape Memory Alloy Actuators *Cdn.Intechweb.Org* 107–27

[40]   Tung A T, Park B H, Koolwal A, Nelson B, Niemeyer G and Liang D 2006 Design and fabrication of tubular shape memory alloy actuators for active catheters *Proceedings of the First IEEE/RAS-EMBS International Conference on Biomedical Robotics and Biomechatronics, 2006, BioRob 2006* vol 2006pp 775–80

[41]   Veeramani A S, Buckner G D, Owen S B, Cook R C and Bolotin G 2008 Modeling the dynamic behavior of a shape memory alloy actuated catheter *Smart Mater. Struct. Smart Mater. Struct* **17** 1–4

[42]   Crews J H and Buckner G D 2012 Design optimization of a shape memory alloy-actuated robotic catheter *J. Intell. Mater. Syst. Struct.* **23** 545–62

[43]   Ayvali E, Liang C-P, Ho M, Chen Y and Desai J P 2012 Towards a discretely actuated steerable cannula for diagnostic and therapeutic procedures *Int. J. Rob. Res.* **31** 588–603

[44]   Frank T G, Xu W and Cuschieri A 2000 Instruments based on shape- memory alloy properties for minimal access surgery, intenrentional radiology and flexible endoscopy *Minim. Invasive Ther. Allied Technol. ISSN* **9** 89–98

[45]   Reynaerts D and Brussel H Van 1998 Design aspects of shape memory actuators *Mechatronics* **8** 635–56

[46]   Guo Z, Pan Y, Wee L B and Yu H 2015 Design and control of a novel compliant differential shape memory alloy actuator *Sensors Actuators, A Phys.*

[47]   Miller D A and Lagoudas D C 2000 Thermomechanical characterization of NiTiCu and NiTi SMA actuators: influence of plastic strains *Smart Mater. Struct.* **9** 640–52

[48]   Lee J H, Park J B, Andreasen G F and Lakes R S 1988 Thermomechanical study of Ni-Ti alloys. *J. Biomed. Mater. Res.* **22** 573–88

[49]   ASTM Int. 2009 Standard Test Method for Transformation Temperature of Nickel-Titanium Alloys by thermal analysis *Annu. B. ASTM Stand.* **5** 7–10

[50]   Choi E, Lee D-H and Choei N-Y 2009 Shape Memory Alloy Bending Bars as Seismic Restrainers for Bridges in Seismic Areas *Steel Struct.* **9** 261–73

[51]   Sofla A Y N, Elzey D M and Wadley H N G 2008 Cyclic degradation of antagonistic shape memory actuated structures *Smart Mater. Struct.* **17** 025014 (6)

[52]   Robertson S W, Pelton A R and Ritchie R O 2012 Mechanical fatigue and fracture of Nitinol *Int. Mater. Rev.* **57** 1–37

[53]   Gall K and Maier H J 2002 Cyclic deformation mechanisms in precipitated NiTi shape memory alloys *Acta Mater.* **50** 4643–57

[54]   Orgéas L and Favier D 1998 Stress-induced martensitic transformation of a NiTi alloy in isothermal shear, tension and compression *Acta Mater.* **46** 5579–91

[55]   Eggeler G, Hornbogen E, Yawny A, Heckmann A and Wagner M 2004 Structural and functional fatigue of NiTi shape memory alloys *Mater. Sci. Eng. A* **378** 24–33

[56]   Hornbogen E 2002 Some effects of martensitic transformation on fatigue resistance *Fatigue Fract. Eng. Mater. Struct.* **25** 785–90

[57]   ASTM Int. 2016 Standard Test Method for Determination of Transformation Temperature of Nickel-Titanium Shape Memory Alloys by Bend and Free Recovery *Annu. B. ASTM Stand.* 1–7

[58]   Lexcellent C and Bourbon G 1996 Thermodynamical model of cyclic behaviour of Ti-Ni and Cu-Zn-Al shape memory alloys under isothermal undulated tensile tests *Mech. Mater.* **24** 59–73

VITA

Ali Vahidyeganeh was born and raised in Tehran, Iran. He went on to continue his academic education in University of Tehran, Iran, where he obtained a BS in mechanical engineering in September of 2012. His bachelor's project was focusing on the design of mechanism for a retractable tensile structure. Upon graduation, Ali moved his studies to Istanbul to participate a comprehensive research project on smart materials in MEMFIS group under the supervision of Dr. Yapıcı. While contributing to MEMFIS, he has been working towards his MS degree in Mechanical Engineering at Ozyegin University.